Electronic Supplementary Material (ESI) for Journal of Materials Chemistry A.

Supplementary information

Mechanisms of and three-dimensional morphology changes in fluoride shuttle battery reactions of PbF_2 microparticles

Toshiro Yamanaka,[*a] Zempachi Ogumi,[a] and Takeshi Abe[b]

[a]*Office of Society-Academia Collaboration for Innovation, Kyoto University, Katsura, Nishikyo, Kyoto 615-8530, Japan.*

[b]*Graduate School of Global Environmental Studies, Kyoto University, Katsura, Nishikyo, Kyoto 615-8510, Japan*

[*]e-mail: yamanaka.toshiro.8n@kyoto-u.ac.jp

1. Gold foil without PbF_2 that was kept at -0.25 V

In the present study, a Pb wire was used as a reference electrode. To confirm that bright blue Pb particles shown in Figs. 4f (blue arrows) and 8c (the green line) in the main text did not come from the Pb reference electrode, a cell was assembled by using a gold working electrode without PbF_2 microparticles. Figure S1a shows a CCD image of the gold sample at OCV (0.5 V) in the cell taken just after the cell had been constructed. Figure S1b shows a CCD image of the sample after E_{WE} had been kept at -0.25 V for five days, and no Pb particles were observed. The results indicate that the blue particles were not from the Pb reference electrode.

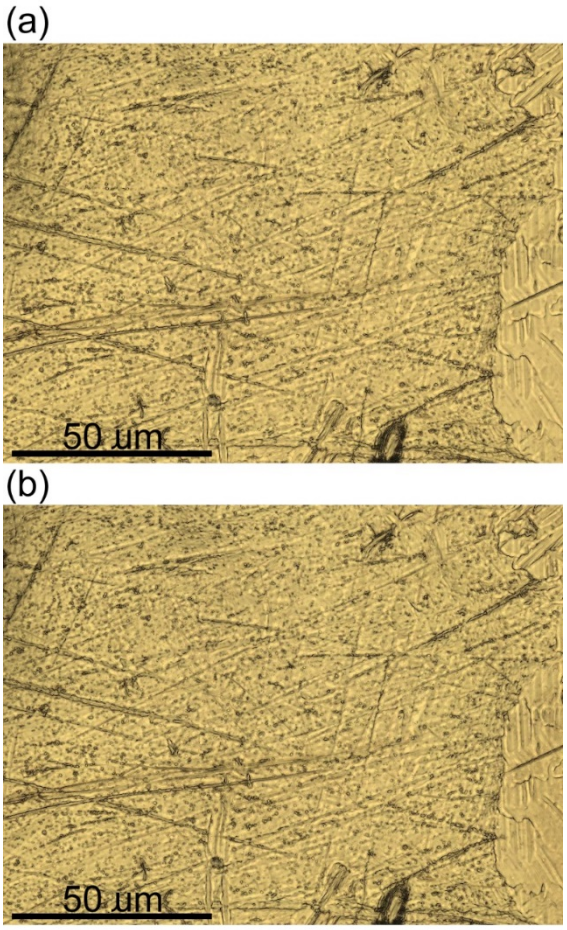

Fig. S1 Gold foil without PbF_2 that was kept at -0.25 V: (a) and (b) show CCD images of the gold sample without PbF_2 microparticles at OCV and after E_{WE} had been kept at -0.25 V for five days.

2. XRD patterns of c-PbF_2/gold before and after defluorination

Figure S2a shows an XRD pattern of c-PbF_2/gold taken in air before it was set in an electrochemical Raman cell. Two peaks were observed, which agree with the XRD peaks of c-PbF_2 in the database shown in Fig. S2b. The cell was constructed using a c-PbF_2/gold sample, and defluorination of c-PbF_2 was induced by keeping E_{WE} at -0.25 V for one week. An XRD pattern of the resultant sample was measured without exposing the sample to air, and the XRD pattern is shown in Fig. S2c. Only two peaks that agree with XRD peaks of Pb in the database (Fig. S2d) were observed, indicating that defluorination of c-PbF_2 on the c-PbF_2/gold sample occurred.

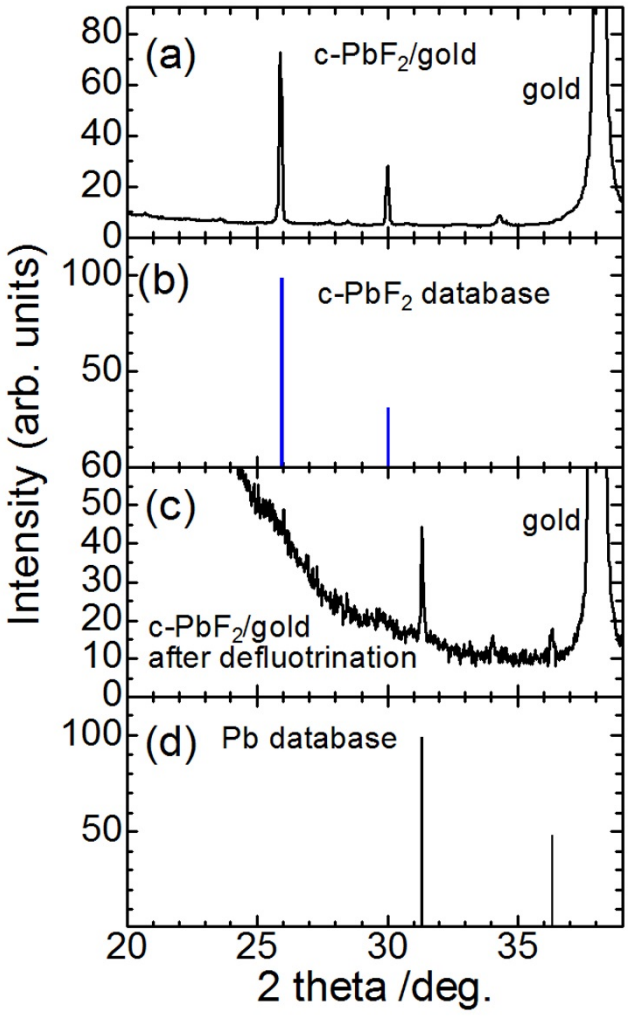

Figure S2. XRD patterns of a c-PbF_2/gold sample before (a) and after (c) defluorination with XRD patterns of c-PbF_2 in the database (b) and Pb in the database (d).

3. Experimental setup

Figure S3a shows an outline of electrochemical cell and Ar flow. The cell was assembled in an Ar atmosphere in a glove box. Since the amount of PbF_2 is very small, it is difficult to obtain the OCV of a PbF_2/gold sample. When the sample was mounted on a stainless current collector in the electrolyte, the value of OCV often showed the potential of stainless, not PbF_2. Therefore, the use of a stainless current collector was avoided to measure OCV that reflects the potential of PbF_2. The amount of the electrolyte was also minimized considering the small amount of PbF_2. As shown in Fig. S3b, a gold foil had a protrusion with a height of about 0.95 mm and PbF_2/gold was prepared on the protrusion (See supplementary information of a previous paper (Journal of The Electrochemical Society, 166 (4) A635-A640 (2019).). The resultant sample was put on a PEEK base. A Kalrez o-ring with a thickness of 1 mm was put around the protrusion of the gold foil. The o-ring was filled with the electrolyte and a quartz window attached to a PEEK flange was put on it. The PEEK base was put in an argon chamber, and the inner lid and an outer lid were closed. Then the argon chamber was taken out from the glove box and Ar flow was started. Then the outer lid was taken off and the argon chamber was put on the sample stage of a Raman or LSCM apparatus (Fig. S4). The argon chamber was replaced between the stages of the two apparatuses, as shown in Fig. S4.

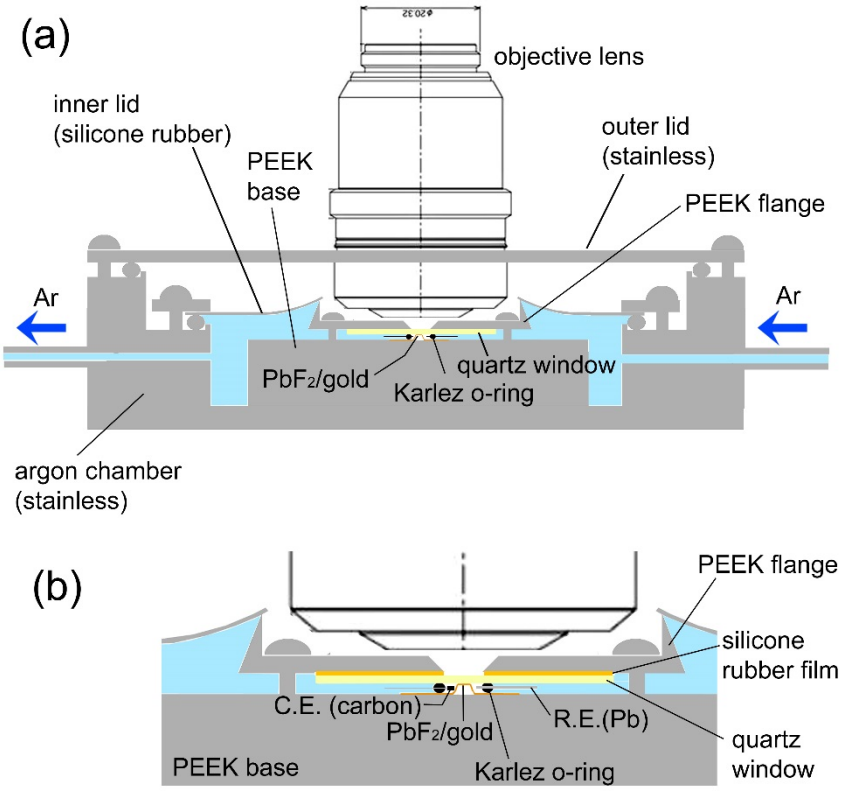

Fig. S3 Outline of the electrochemical cell and Ar flow.

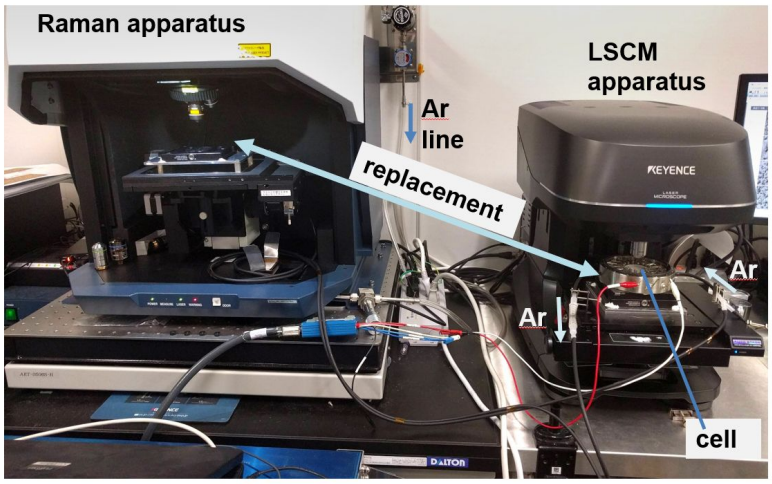

Fig. S4 Raman and LSCM apparatuses.

A more detailed procedure of setup is shown below. Three pieces of stamp (Fig. S5a) were used to make the protrusion of the gold foil (Fig. S5b).

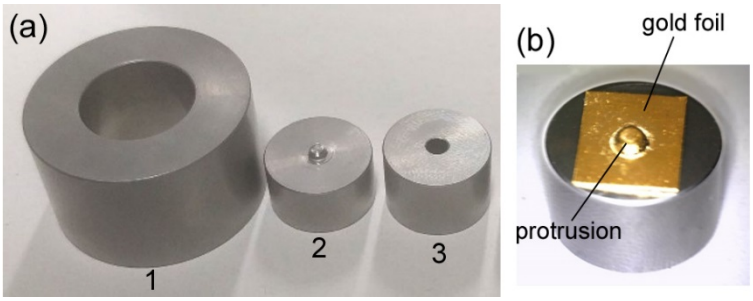

Fig. S5 Stamp made of steel used to make a protrusion of the gold foil.

Three side holes were made on the Karlez o-ring, and the Pb reference electrode and a sus316 wire were inserted into the o-ring from the side holes as shown in Fig. S6. The carbon composite sheet was clipped to the sus316 wire using a sus316 plate.

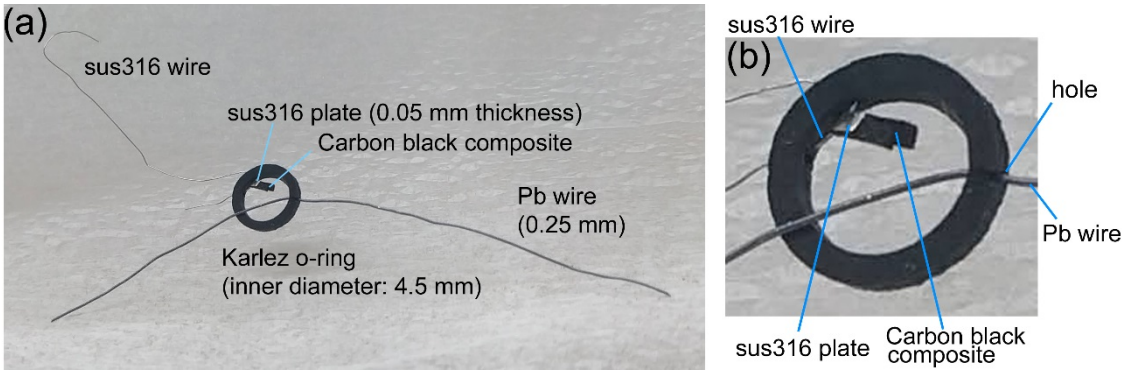

Fig. S6 Details of the o-ring, reference and counter electrodes.

The gold foil was put on the PEEK base, and a polyimide film insulator was put around the protrusion of gold to avoid contact between the three electrodes, as shown in Fig. S7a. The shape of the insulator is indicated by a brown color. The Pb wire attached to the o-ring (Fig. S6) was cut and shortened and the tip of the wire was polished to eliminate PbO at the surface of the Pb wire. Then the o-ring was put around the PbF_2/gold (protrusion of the gold foil). Several droplets of electrolyte were dropped in the o-ring, and a quartz window with a PEEK flange was put on the o-ring (Fig. S7b and S7c). If there was a bubble of Ar in the electrolyte inside the o-ring, it was driven out by moving the window up and down, a procedure that may need some practice. The PEEK flange was then fixed by four screws (Fig. S7c). Electrolyte outside the o-ring was eliminated by inserting a piece of paper filter between the PEEK flange and the PEEK base.

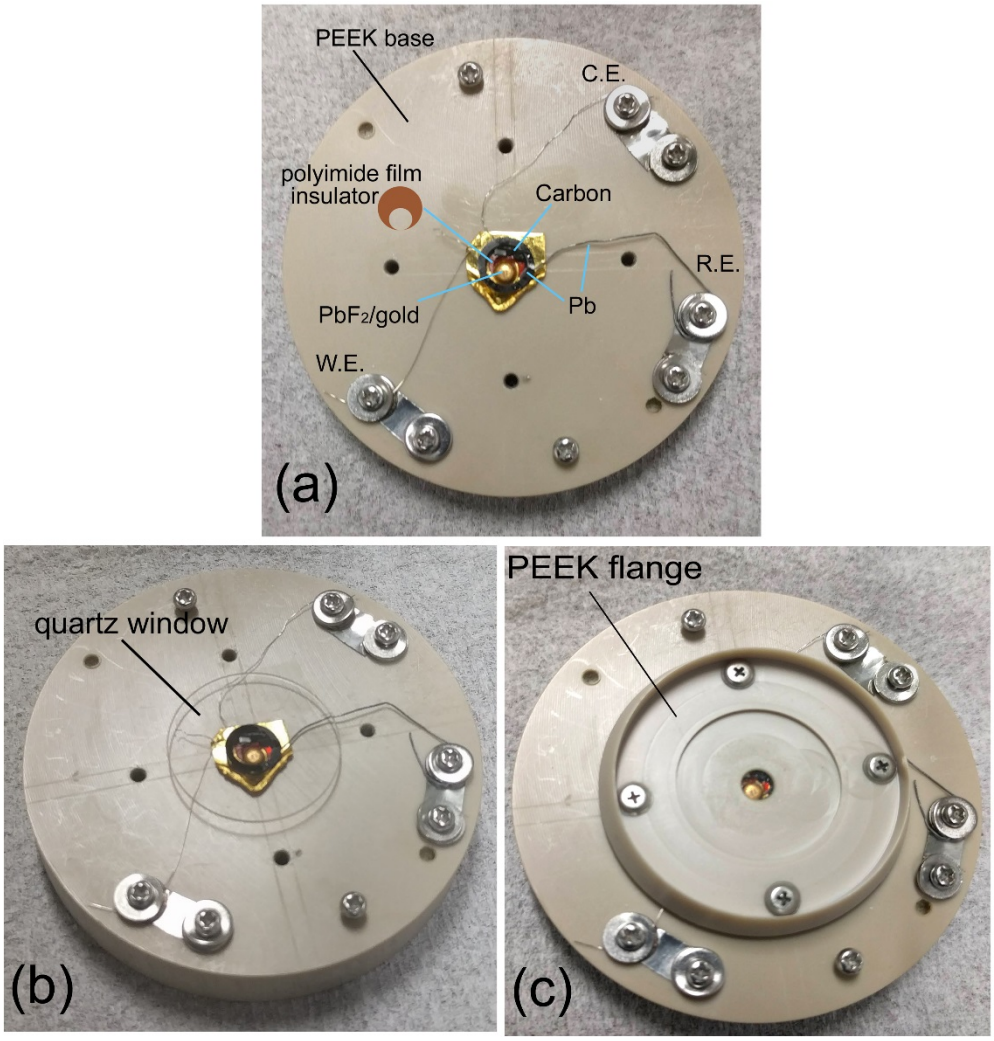

Fig. S7 An electrochemical cell made on a PEEK base.

The PEEK base was put in the argon chamber (Fig. S8a) and the inner lid was put on them. The inner lid was made of a thin silicone rubber film so that it can be flexibly adjusted to various heights of electrochemical cells on the PEEK base, of which the design is often changed depending on experiments. The silicone rubber film was fixed to the PEEK flange by using many screws (Fig. S8b) depending on the height of the flange. However, the sealing between the flange and silicone rubber film may not be sufficient without Ar flow. Therefore, the outer lid was used for sufficient sealing (Fig. S8c) before the Ar flow was started. Then the argon chamber was taken out from the glove box. After the Ar flow had been started, the outer lid was removed. Areas of PbF_2/gold around the center of the protrusion on the gold foil were studied by Raman mapping and LSCM.

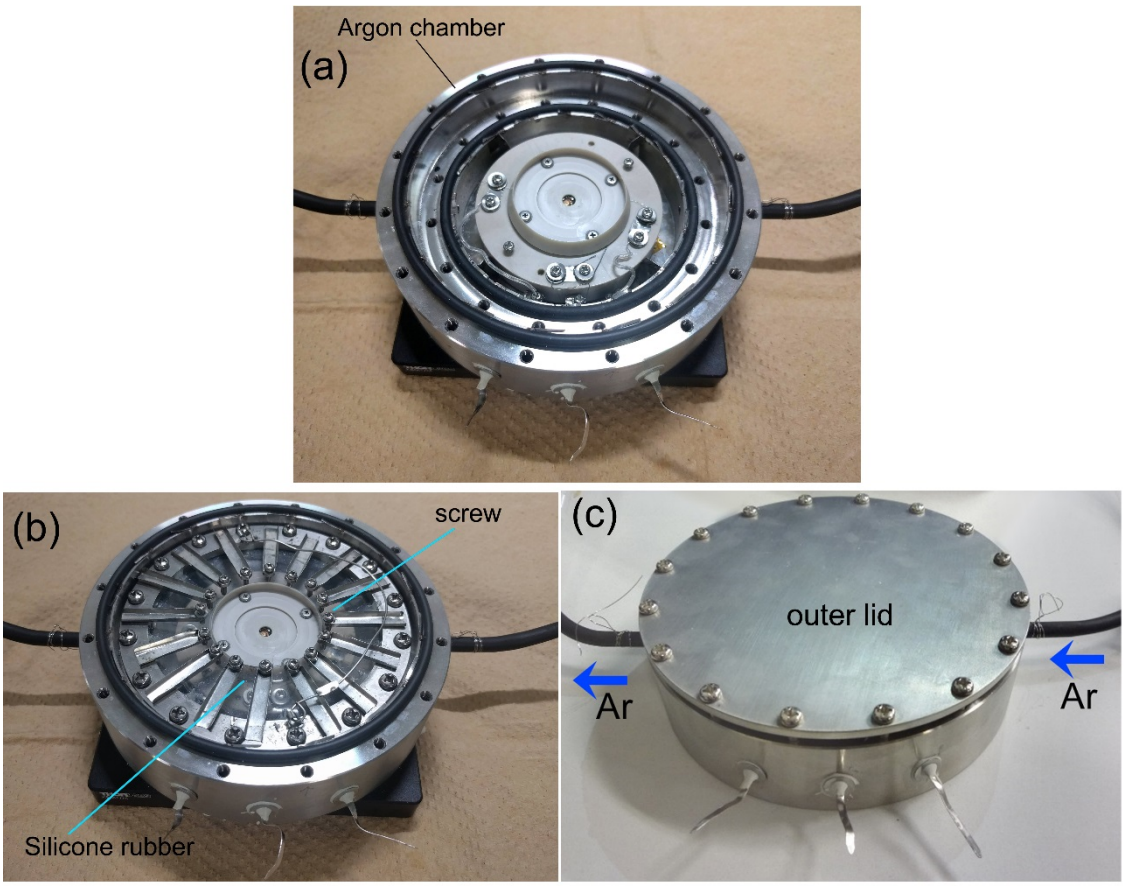

Fig. S8 The electrochemical cell set in the argon chamber.

4. Height profiles and starting positions of F^- desorption

The correlation between protrusions on the surfaces of o-PbF_2 and c-PbF_2 particles and positions where desorption of F^- started (judged from the darkened color) was further studied. Figures S9a-9c show defluorination of o-PbF_2 in the same area as those in Fig. 5 in the main text. Defluorination started at the positions indicated by 1, 2, 3 and 4 in Fig. S9b. Height profiles along lines P-Q, R-S, T-U and V-W that include the points 1, 2, 3 and 4, respectively, are shown in Fig. S9d, S9e, S9f and S9g, respectively. The points 1, 2, 3 and 4 coincide with protrusions, suggesting that the rate-determining step of defluorination by desorption of F^- is extraction of F^- from the surface of o-PbF_2 into the electrolyte. However, the sizes of spots where defluorination started seem large and blurred compared to those observed in a previous work (ACS appl. energy mater. 2, 3092 (2020)), suggesting that extraction of F^- is not a strong and sole rate-determining step and it may compete with other steps, such as nucleation of metal Pb.

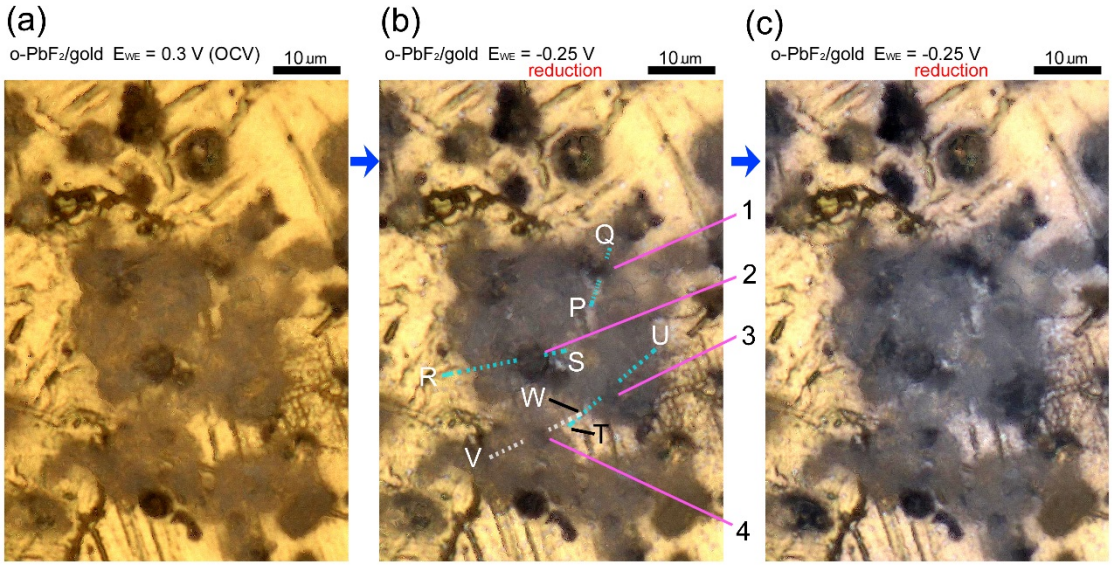

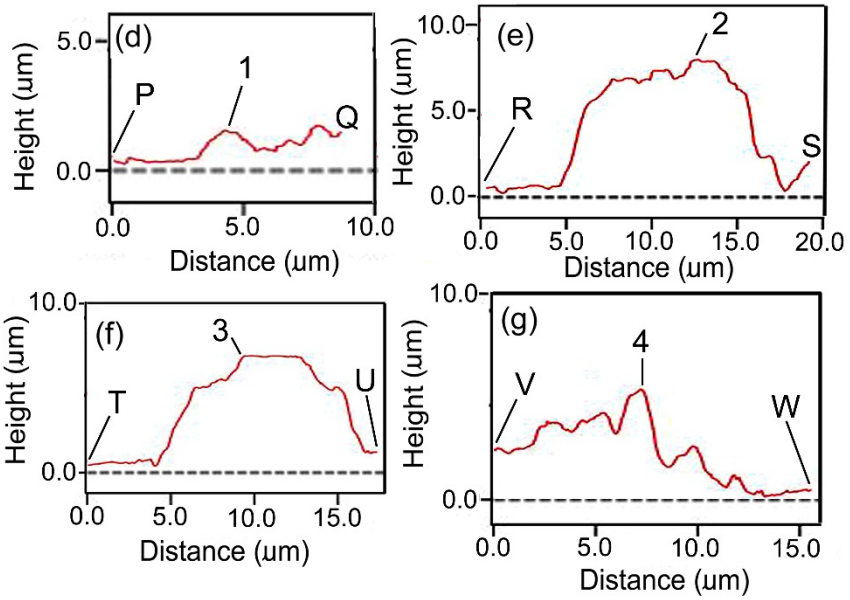

Fig. S9 Correlation between protrusions on the surfaces of o-PbF_2 particles and positions where defluorination by desorption of F^- starts. (a)-(c) show LSCM images during defluorination. (d), (e), (f) and (g) show height profiles along lines P-Q, R-S, T-U and V-W shown in (b).

Figures S10a-10c show defluorination of c-PbF_2 in the same area as those in Fig. 9 in the main text. Defluorination started at the positions indicated by 1, 2 and 3 in Fig. S10b. Height profiles along lines P-Q, R-S and T-U that include the points 1, 2 and 3, respectively, are shown in Fig. S10d, S10e and S10f, respectively. The points 1, 2 and 4 coincide with protrusions, suggesting that the rate-determining step of defluorination by direct desorption is extraction of F^- from the surface of c-PbF_2 into the electrolyte. The spots where defluorination started seem large and blurred compared to those observed in a previous work (ACS appl. energy mater. 2, 3092 (2020)), suggesting that extraction of F^- is not a strong rate-determining step.

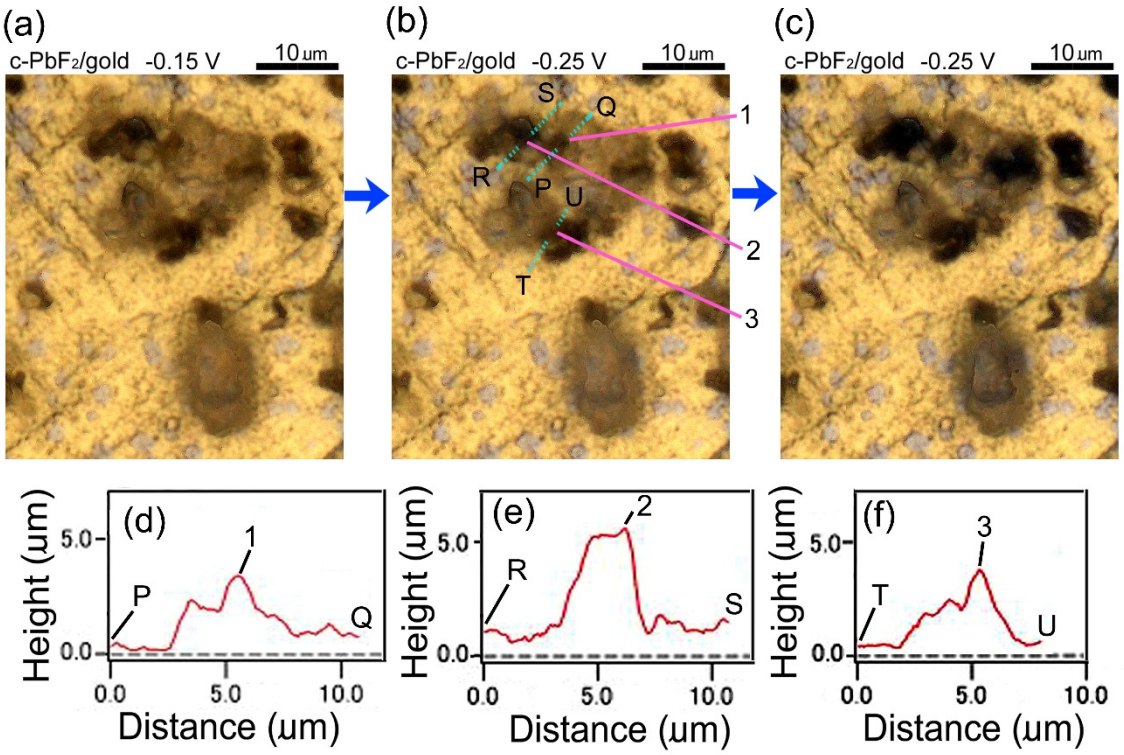

Fig. S10 Correlation between protrusions on the surfaces of c-PbF_2 particles and positions where defluorination by the direct desorption mechanism starts. (a)-(c) show LSCM images during defluorination. (d), (e) and (f) show height profiles along lines P-Q, R-S and T-U shown in (b).

5. SEM-EDS of o-PbF_2/gold and c-PbF_2/gold after applying voltages in electrochemical cells

Considering results of Raman and LSCM measurements, defluorination mechanisms shown in Fig. 10 in the main text were suggested. These mechanisms were proposed mainly on the basis of color of confocal CCD images, and the mechanisms should be studied by additional methods. Thus we conducted ex-situ SEM-EDS experiments of o-PbF_2/gold and c-PbF_2/gold samples before and after defluorination.

5-1 o-PbF_2/gold after being kept at OCV

An electrochemical cell was assembled with a new o-PbF_2/gold sample and the electrolyte, and the sample was kept at OCV for three days. Then the sample was taken out and SEM-EDS measurements were conducted. Figure S11 shows results of SEM-EDS measurements. It is shown that F and Pb existed only at the positions of particles, which are thought to be o-PbF_2 particles, not on the gold substrate.

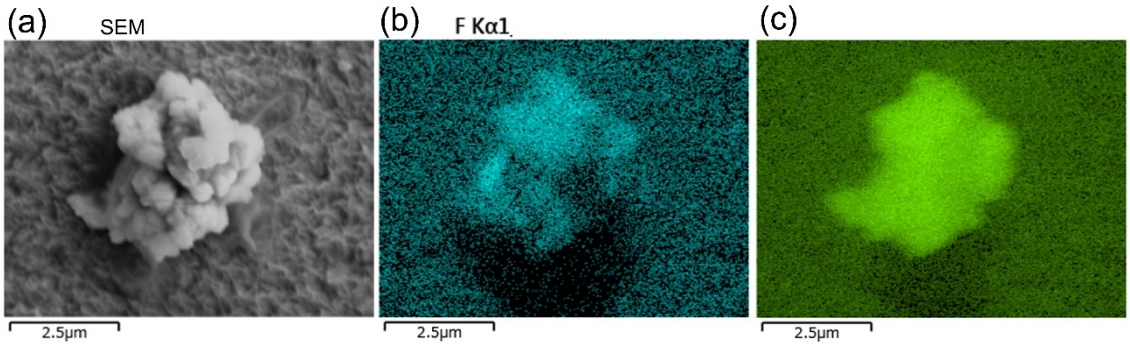

Fig. S11 Results of SEM-EDS measurements of o-PbF_2/gold after being kept at OCV for three days.

5-2 o-PbF_2/gold after being kept at -0.05 V vs Pb

An electrochemical cell was assembled using a new o-PbF_2/gold sample, and the sample was kept at OCV for three days to induce chemical dissolution of o-PbF_2. Figure S12a shows a confocal CCD image of o-PbF_2/gold after it was kept at OCV for three days. A zoomed image of the area indicated by the blue rectangle in (a) is shown in (b). Then the sample was kept at -0.05 V vs Pb for four hours, and white blue particles, which are thought to be Pb particles, appeared as shown in (c). A zoomed image of the area indicated by the blue rectangle in (c) is shown in (d). Blue arrows in (d) indicate white blue particles.

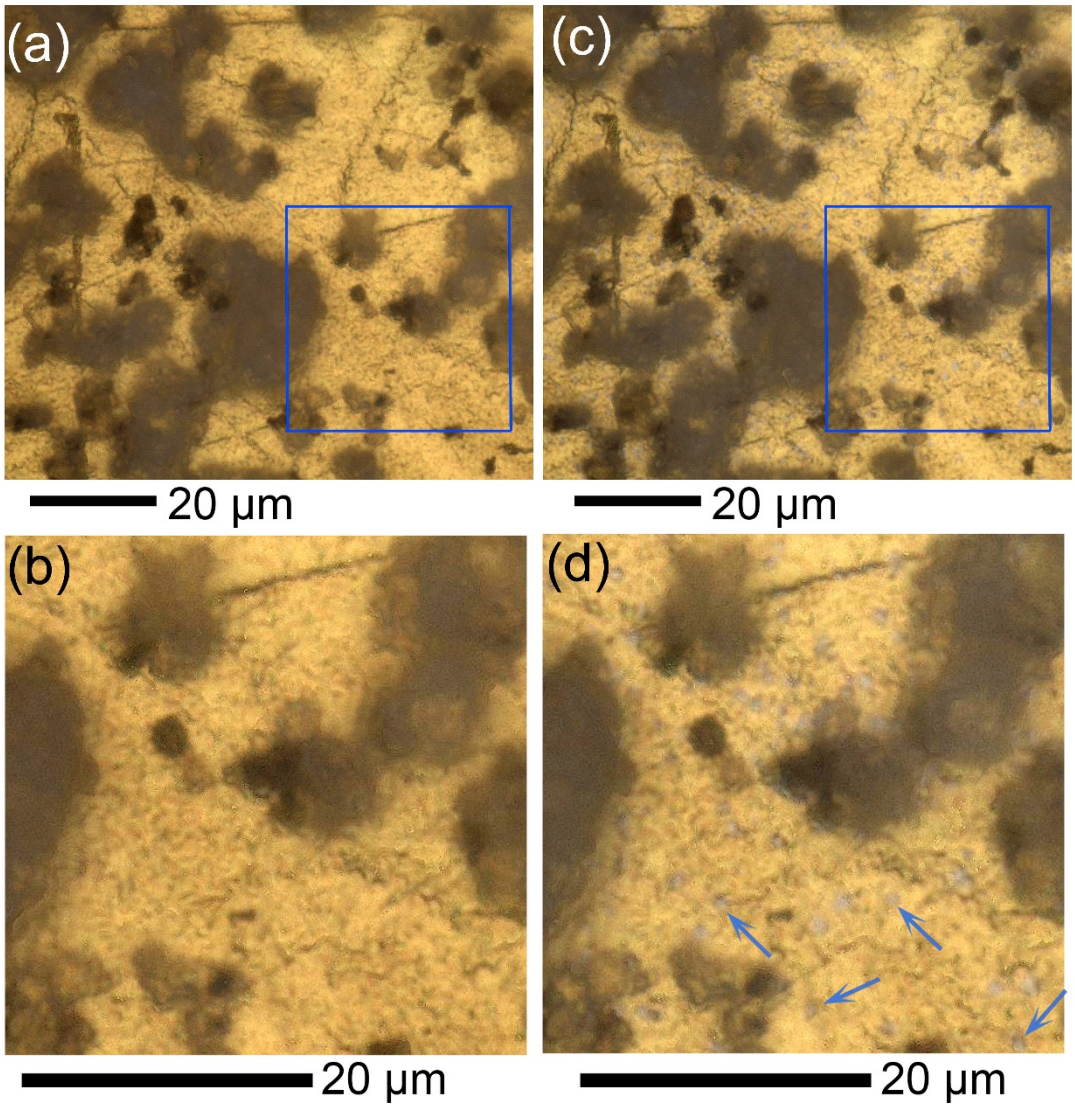

Fig. S12 Confocal CCD images of o-PbF_2/gold after being kept at OCV for three days ((a) and (b)) and at -0.05 V vs Pb for four hours ((c) and (d)).

The o-PbF_2/gold sample shown in Figs. S12c and S12d was taken out from the electrochemical cell and transferred to an SEM-EDS column, and SEM-EDS

measurements were conducted. An SEM image (Fig. S13a) shows two large particles indicated by white arrows, which are thought to be o-PbF_2 particles, and many fine particles indicated by blue lines. Mappings of F Kα (Fig. S13b) and PbMα (Fig. S13c) indicate that the large particles consisted of both F and Pb and that fine particles consisted of only Pb. Thus, fine particles are thought to be Pb particles produced by the dissolution-deposition mechanism. Thus, the particles indicated by blue arrows in Fig. 4f in the main text are thought to be Pb particles. This agrees with the dissolution-deposition shown in Fig. 10a in the main text.

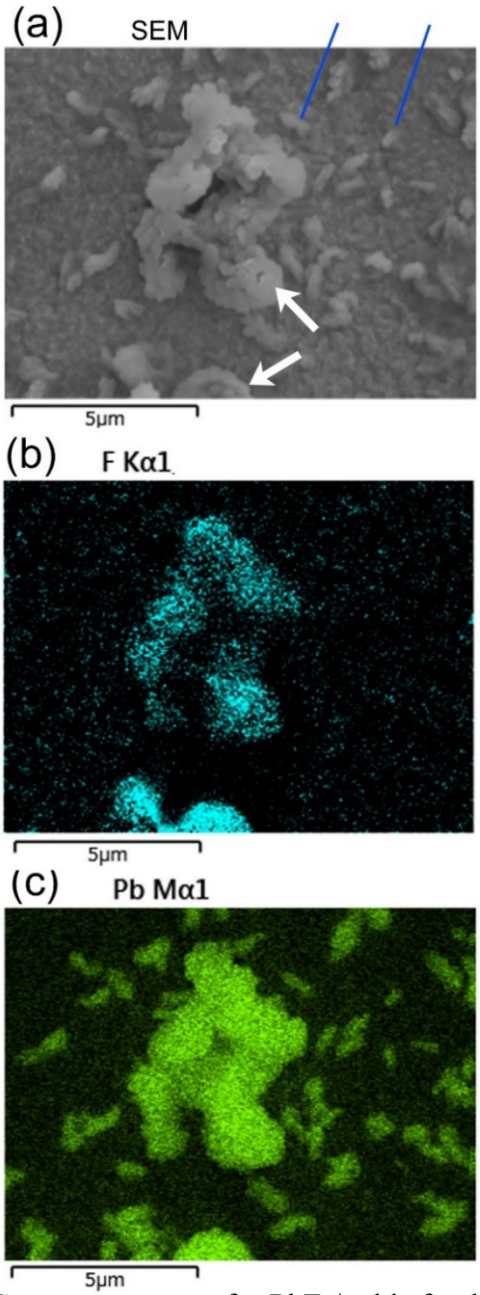

Fig. S13 Results of SEM-EDS measurements of o-PbF_2/gold after being kept at OCV for three days and at -0.05 V vs Pb for four hours.

5-3 o-PbF_2/gold after being kept at -0.25 V vs Pb

An electrochemical cell was assembled using a new o-PbF_2/gold sample. Figures S14a and S14b show confocal CCD images of o-PbF_2/gold just after the cell was assembled and it was kept at OCV for two days and at -0.25 V for four hours to induce desorption of F^- from o-PbF_2 particles. The color of many o-PbF_2 particles in (b) became darker than those in (a), indicating that desorption of F^- had proceeded. Many grey areas appeared around the particles, suggesting that desorption-induced dissolution and subsequent deposition of Pb near the particles had proceeded. This was not observed in Fig. S12c and S 12d after being kept at -0.05 V.

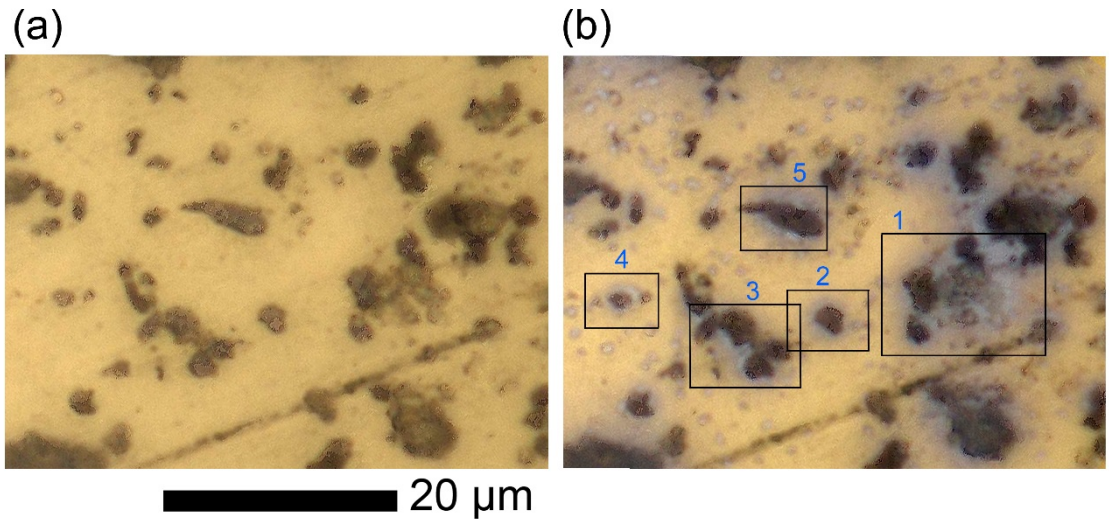

Fig. S14 Confocal CCD images of o-PbF_2/gold just after the cell was assembled (a) and after being kept at -0.25 V for four hours (b). The areas indicated by rectangles 1-5 were chosen for SEM-EDS measurements conducted later.

The sample shown in Fig. S14b was taken out from the electrochemical cell and transferred to an SEM-EDS column, and SEM-EDS measurements were conducted. Results for areas indicated by 1, 2, 3, 4 and 5 in Fig. S14b are shown in Figs. S15a-S15c, S15d-S15f, S15g-S15i S15j-S15l and S15m-S15o, respectively. Generally, the areas of F-rich parts are smaller than the particles observed in SEM images, indicating that desorption of F^- had proceeded. On the other hand, the mappings for Pb show that the areas of Pb-rich parts are larger than the particles observed in SEM images, which is clear in Figs. S15j, S15l, S15m and S15o, as indicated by white-blue lines. Note that the sizes of large particles in the SEM image in Fig. S13a and the corresponding Pb-rich area in Fig. S13c are very similar. The results shown in Figs. S14 and S15 agree with the desorption-induced dissolution and subsequent deposition of Pb shown in Fig. 10c in the main text.

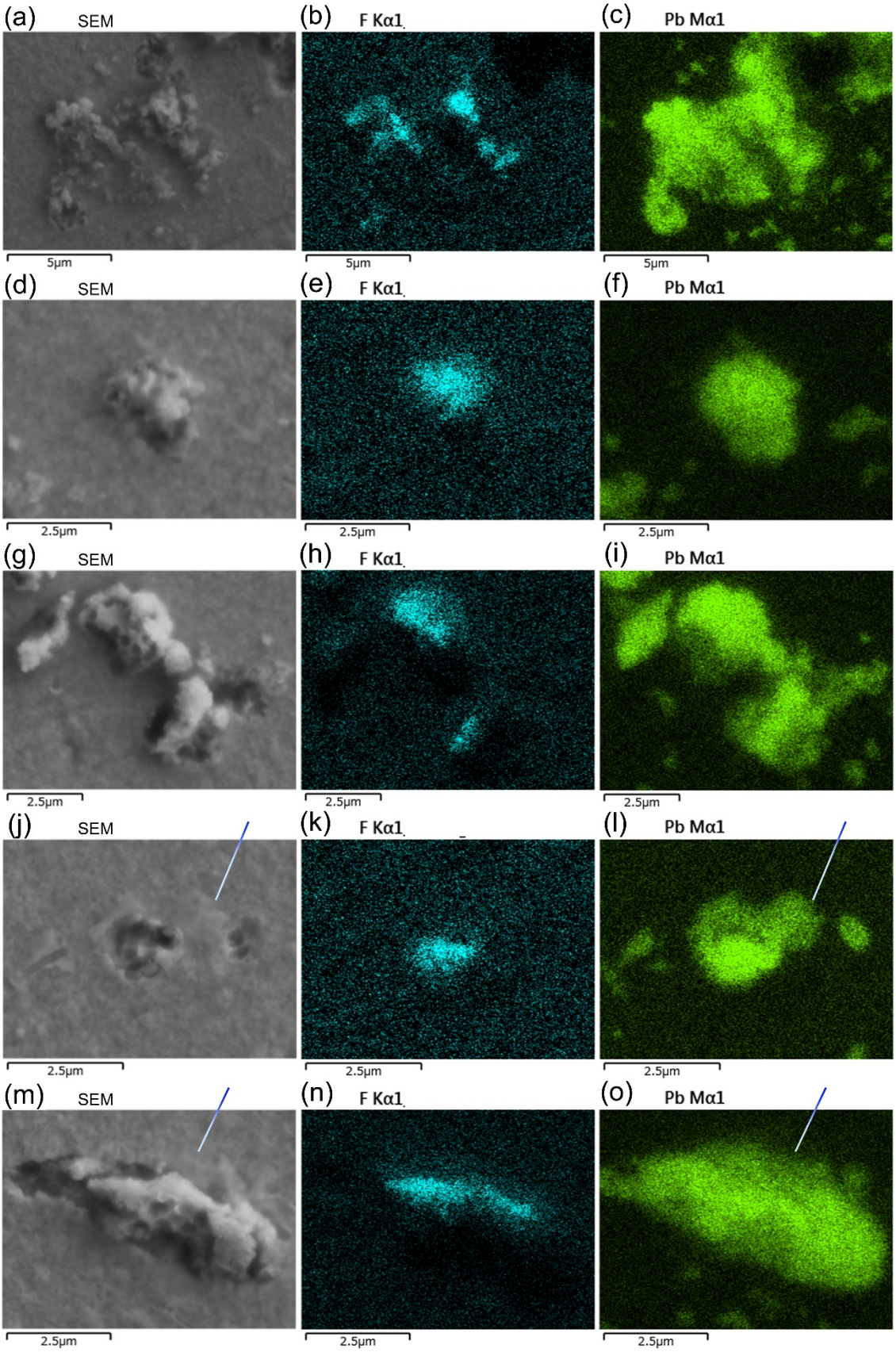

Fig. S15 Results of SEM-EDS measurements of o-PbF_2/gold after being kept at -0.25 V. (a)-(c), (d)-(f), (g)-(i), (j)-(l) and (m)-(o) show results for areas indicated by 1, 2, 3, 4 and

5 in Fig. S14b, respectively.

5-4 c-PbF_2/gold after being kept at OCV

An electrochemical cell was assembled with a new c-PbF_2/gold sample and the electrolyte, and the sample was kept at OCV for three days. Then the sample was taken out and SEM-EDS measurements were conducted. Figure S16 shows results of SEM-EDS measurements. It is shown that F and Pb existed only at the positions of particles, which are thought to be c-PbF_2 particles, not on the gold substrate.

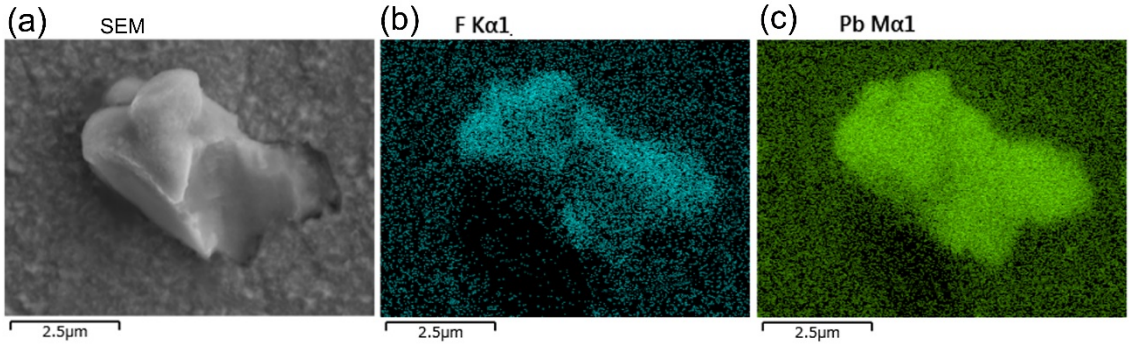

Fig. S16 Results of SEM-EDS measurements of c-PbF_2/gold after being kept at OCV for three days.

5-5 c-PbF_2/gold after being kept at -0.05 V vs Pb

An electrochemical cell was assembled using a new c-PbF_2/gold sample, and the sample was kept at OCV for three days to induce chemical dissolution of c-PbF_2. Figure S17a shows a confocal CCD image of c-PbF_2/gold after it was kept at OCV for three days. Then the sample was kept at -0.05 V vs Pb for four hours, and many particles, which are thought to be Pb particles, appeared as shown in (b).

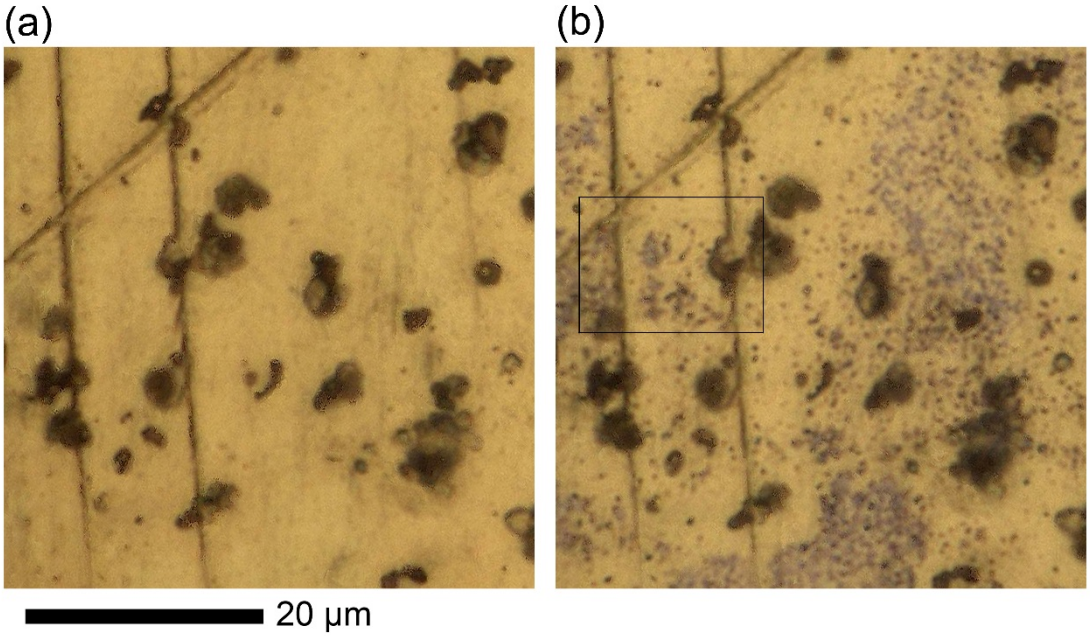

Fig. S17 Confocal CCD images of c-PbF_2/gold after being kept at OCV for three days (a) and at -0.05 V vs Pb for four hours (b). The area indicated by a rectangle was chosen for SEM-EDS measurements conducted later.

The c-PbF_2/gold sample shown in Fig. S17b was taken out from the electrochemical cell and transferred to an SEM-EDS column, and SEM-EDS measurements were conducted. Results for the area indicated by a rectangle in Fig. S17b are shown in Fig. S18. The SEM image (Fig. S18a) shows many fine particles, one of which is indicated by a white-blue line. The mapping of PbMα (Fig. S18c) shows Pb-rich areas at corresponding positions, as indicated by a white-blue line. F-rich areas are not observed at the corresponding positions in the mapping of Fkα (Fig. S18b). Thus, the fine particles are thought to be Pb particles, and also the particles indicated by the green line in Fig. 8c in the main text are thought to be Pb particles. The results agree with the dissolution-deposition shown in Fig. 10a in the main text.

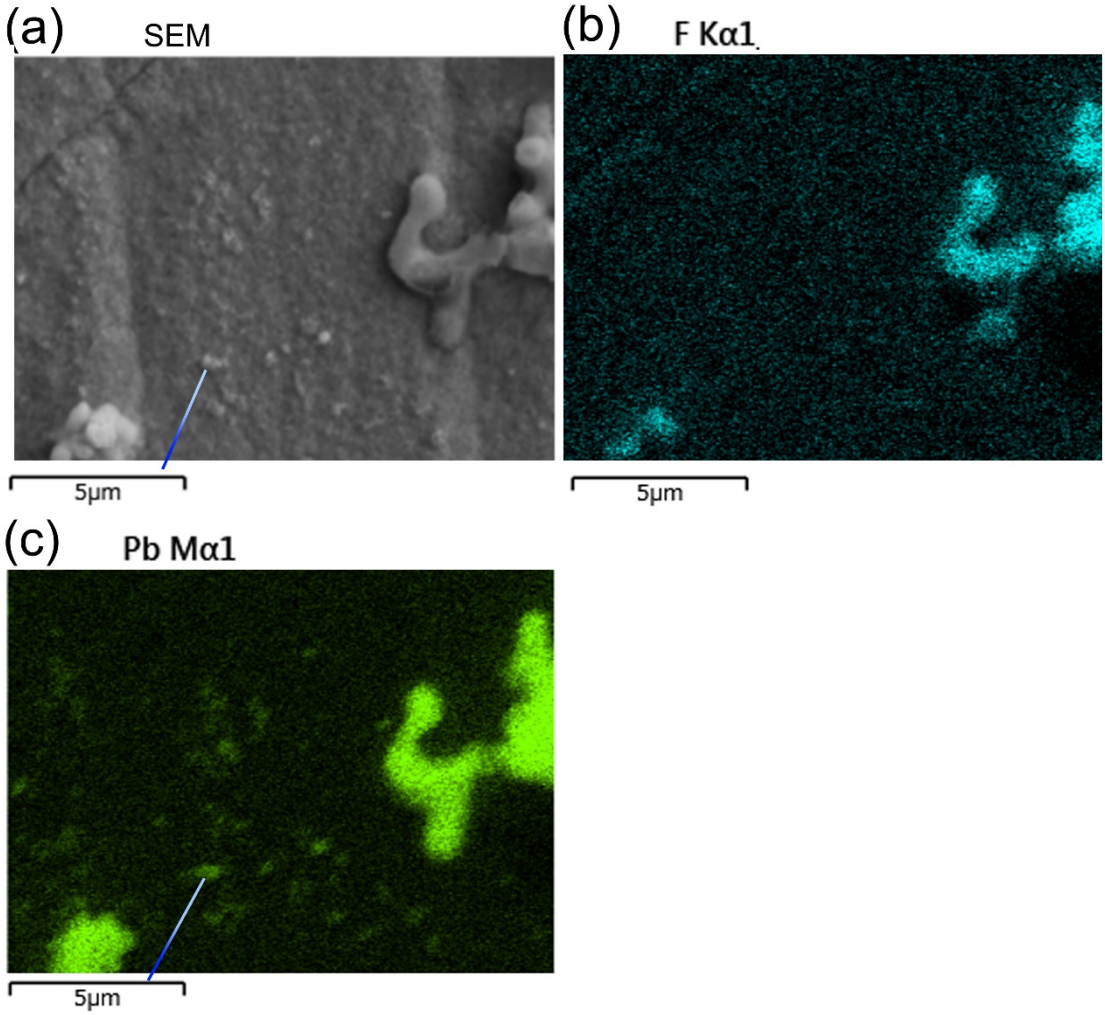

Fig. S18 Results of SEM-EDS measurements of c-PbF_2/gold after being kept at OCV for three days and at -0.05 V vs Pb for four hours.

5-6 c-PbF_2/gold after being kept at -0.25 V vs Pb

An electrochemical cell was assembled using a new c-PbF_2/gold sample. Figures S19a and S19b show confocal CCD images of c-PbF_2/gold just after the cell was assembled and after it was kept at -0.25 V for four hours to induce desorption of F^- from c-PbF_2 particles. The color of many c-PbF_2 particles in (b) became darker than those in (a), indicating that desorption of F^- had proceeded. In (b), grey areas around the particles, which were observed for o-PbF_2/gold in Fig. S14b, were not seen, suggesting that desorption-induced dissolution and subsequent deposition of Pb near the particles had not occurred.

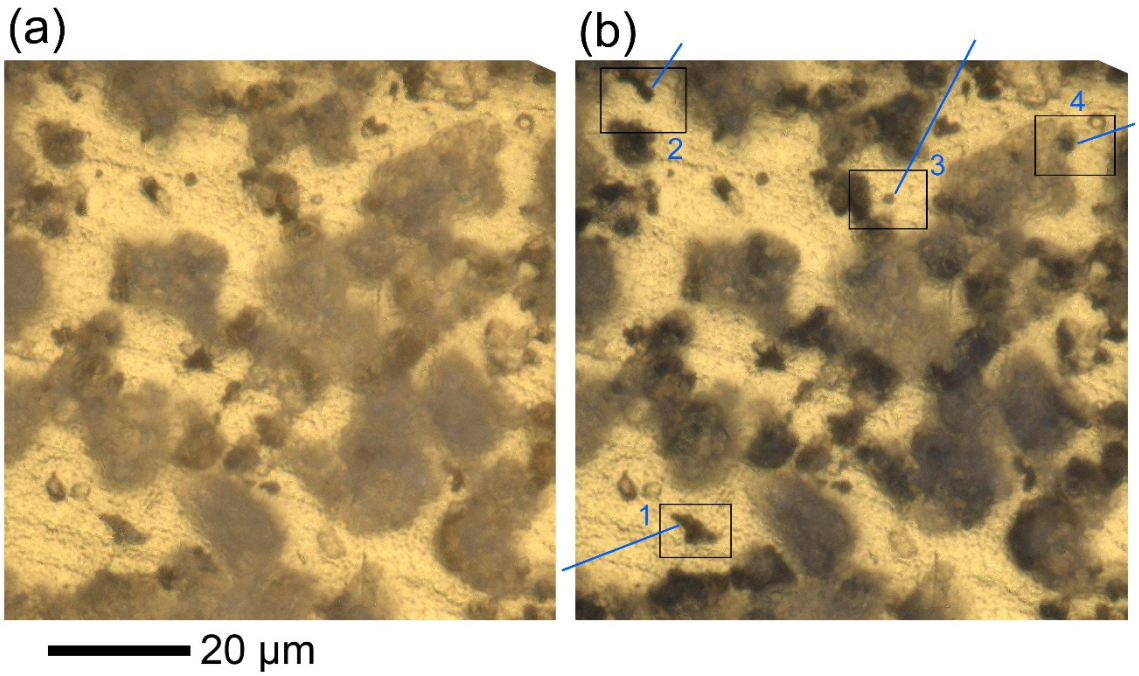

Fig. S19 Confocal CCD images of c-PbF_2/gold just after the cell was assembled (a) and after being kept at -0.25 V for four hours (b). The positions indicated by blue lines in rectangles 1-4 were chosen for SEM-EDS measurements conducted later.

The sample shown in Fig. S19b was taken out from the electrochemical cell and transferred to an SEM-EDS column, and SEM-EDS measurements were conducted. Results for areas indicated by 1, 2, 3 and 4 in Fig. S19b are shown in Figs. S20a-S20c, S20d-S20f, S20g-S20i and S20j-S20l, respectively. The positions indicated by blue lines in Fig. S20 correspond to the positions indicated by blue lines in Fig. S19b, and desorption of F^- had occurred at these positions as indicated by the dark contrasts in Fig. S19b. At these positions, intensities in mappings of F are weak due to defluorination. In Fig. S20, the sizes and shapes of Pb-rich areas are almost the same as those of corresponding parts of particles in SEM images, and contours of Pb-rich areas in the mapping of PbM α are clear, being different from the results for o-PbF_2/gold shown in Fig. S15. These results agree with defluorination by the direct desorption mechanism shown in Fig. 10b in the main text.

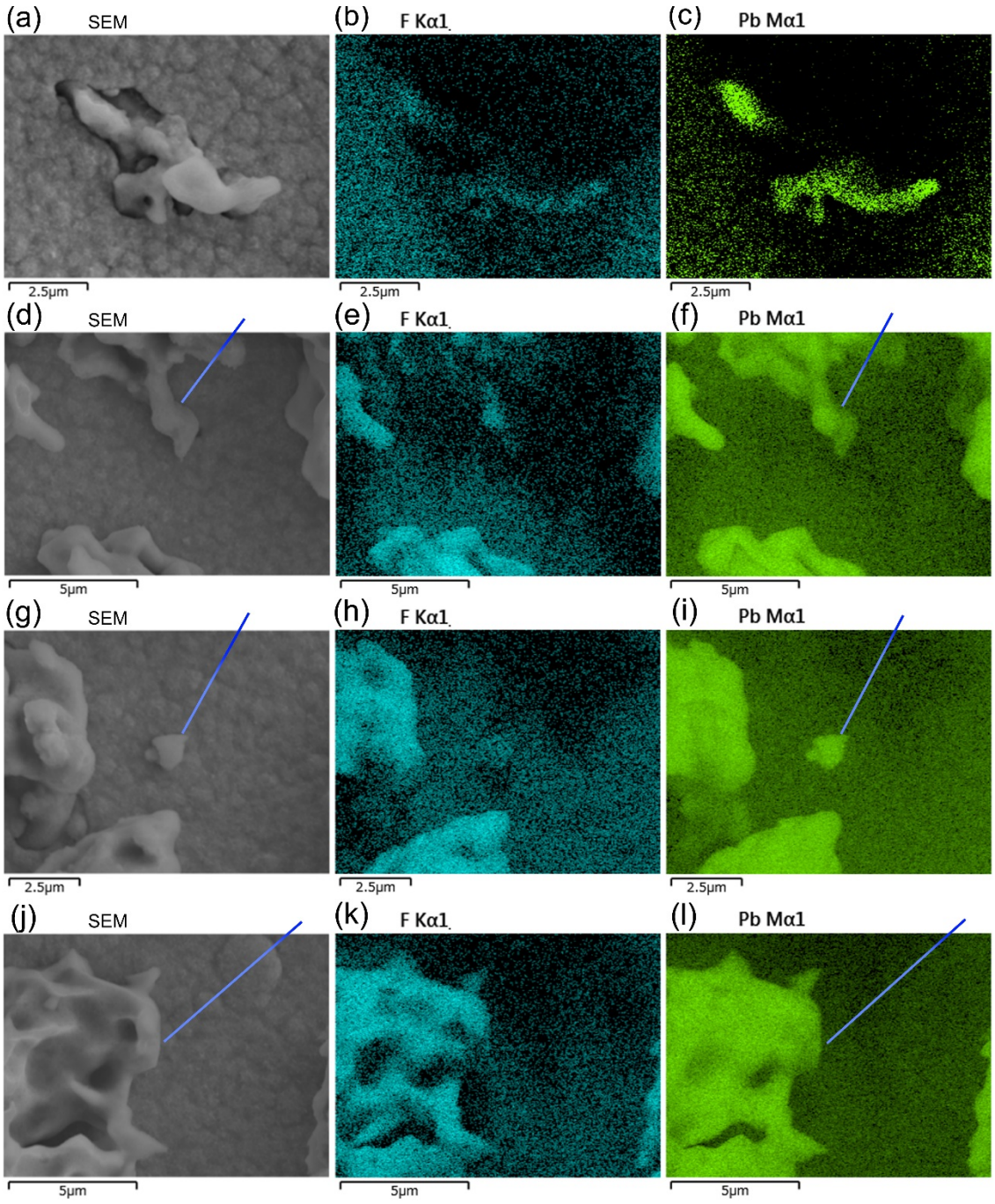

Fig. S20 Results of SEM-EDS measurements of c-PbF_2/gold after being kept at -0.25 V. (a)-(c), (d)-(f), (g)-(i) and (m)-(o) show results for areas indicated by 1, 2, 3 and 4 in Fig. S19b, respectively. The positions indicated by blue lines correspond to those in Fig. S19b.

6. XPS of o-PbF_2/gold and c-PbF_2/gold after being kept at -0.05 V

Small particles were deposited while o-PbF_2/gold and c-PbF_2/gold were kept at -0.05 V as shown by blue arrows in Fig. 4f and a green line in Fig. 8c in the main text, respectively. These particles were thought to be Pb particles based on colors in confocal CCD images and SEM-EDS in sections 5-2 and 5-5 in the supplementary information. To further confirm this, XPS measurements were conducted.

Figure S21a shows an XPS spectrum of Pb4F from a pristine o-PbF_2/gold sample. Two peaks at 139.0 and 143.9 eV are assigned to Pb^{2+} (PbF_2).

An electrochemical cell was assembled using a new o-PbF_2/gold sample. The sample was kept at OCV for three days to induce chemical dissolution of o-PbF_2/gold, and the confocal CCD image shown in Fig. S21b was obtained. Then the sample was kept at -0.05 V vs Pb for four hours, and the confocal CCD image shown in Fig. S21c was obtained. Many fine blue particles are seen as indicated by blue lines. The colors of o-PbF_2 particles in (c) did not become darker compared with those in (b), suggesting that desorption of F^- from o-PbF_2 particles did not occur. This sample was transferred to an XPS chamber without being exposed to air.

Figure S21d shows an XPS spectrum of Pb4F from the o-PbF_2/gold sample after being kept at -0.05 V. In addition to the peak of Pb^{2+}, two new peaks corresponding to metal Pb were observed at 136.6 and 141.5 eV. These results suggest that the fine blue particles shown in (c) are particles of metal Pb, which agree with dissolution deposition shown in Fig. 10a in the main text.

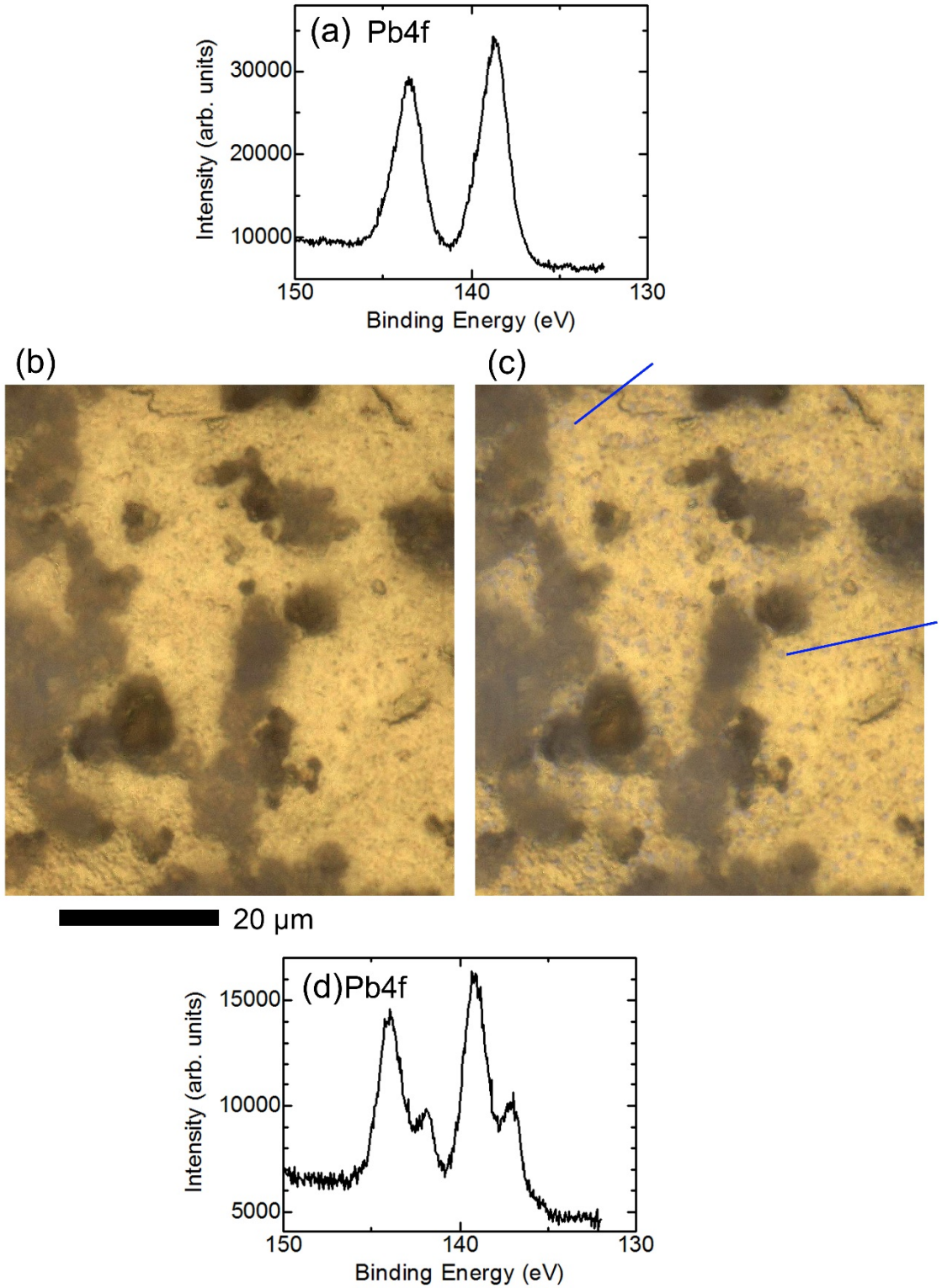

Fig. S21 Results of XPS measurements of o-PbF_2/gold after being kept at -0.05 V. (a) shows an XPS spectrum of Pb4F of a pristine o-PbF_2/gold sample. (b) and (c) show confocal CCD images of o-PbF_2/gold after being kept at OCV for three days and after being kept at -0.05 V for four hours, respectively. (d) shows an XPS spectrum of Pb4F of o-PbF_2/gold after being kept at -0.05 V vs Pb.

Figure S22a shows an XPS spectrum of Pb4F from a pristine c-PbF_2/gold sample. Two peaks corresponding to Pb^{2+} (PbF_2) were seen at 139.0 and 143.9 eV.

An electrochemical cell was assembled using a new c-PbF_2/gold sample. The sample was kept at OCV for three days, and the confocal CCD image shown in Fig. S22b was obtained. Then the sample was kept at -0.05 V vs Pb for four hours, and the confocal CCD image shown in Fig. S22c was obtained. Many fine blue particles appeared as indicated by blue lines. The colors of c-PbF_2 particles in (c) are almost the same as those in (b), suggesting that desorption of F^- from c-PbF_2 particles did not occur. Then the sample was transferred to an XPS chamber without being exposed to air.

Figure S22d shows an XPS spectrum of Pb4F from the c-PbF_2/gold sample after being kept at -0.05 V. In addition to the peak of Pb^{2+}, two peaks were observed at 136.6 and 141.5 eV, and these are assigned as metal Pb. These results suggest that the fine blue particles shown in (c) are particles of metal Pb, which agree with dissolution deposition shown in Fig. 10a in the main text.

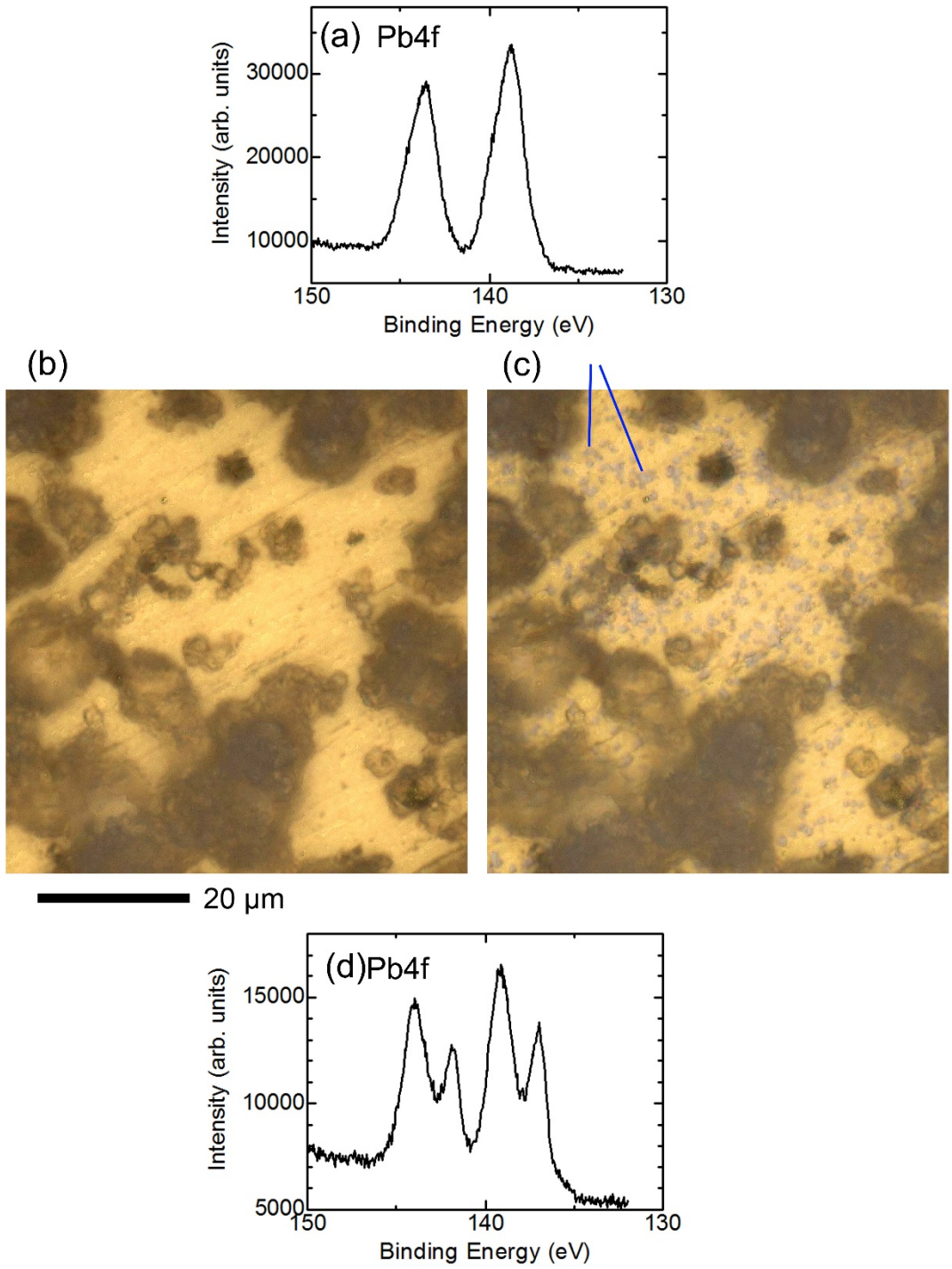

Fig. S22 Results of XPS measurements of c-PbF_2/gold after being kept at -0.05 V. (a) shows an XPS spectrum of Pb4F of a pristine c-PbF_2/gold sample. (b) and (c) show confocal CCD images of c-PbF_2/gold after being kept at OCV for three days and after being kept at -0.05 V for four hours, respectively. (d) shows an XPS spectrum of Pb4F of c-PbF_2/gold after being kept at -0.05 vs Pb.

7. Electrochemical performance test of composite electrodes of o-PbF_2 and c-PbF_2

7-1 Preparation of composite electrodes of o-PbF_2 and c-PbF_2

To determine the effects of defluorination mechanisms of o-PbF_2 and c-PbF_2 on performance of composite electrodes, composite electrodes of o-PbF_2 and c-PbF_2 were prepared and changes in the potential of the electrodes during application of a constant current were studied.

To make composite electrodes of metal fluoride, usually microparticles of metal fluoride provided by a company were ball-milled with carbon black to make a composite of nanoparticles of metal fluoride and carbon (MF_x@C: M being metal). In the case of PbF_2, we found that o-PbF_2 changed to c-PbF_2 during dry ball-milling and that c-PbF_2 changed to o-PbF_2 during wet ball-milling in dehydrated ethanol. Therefore, it is not possible to apply the same ball-milling method to pulverize o-PbF_2 and c-PbF_2. In addition, wet ball-milling generally results in finer particles than does dry ball-milling. It is important to make o-PbF_2@C and c-PbF_2@C with particle sizes as similar as possible and as small as possible.

Considering the above facts, o-PbF_2@C and c-PbF_2@C were made as follows. First, o-PbF_2 (1.6 g) and dehydrated ethanol (5 g) were mixed and ball-milled at 1100 rpm for 2 hours using PL-7 (Fritsch Ltd.), resulting in o-PbF_2 (BM). Then carbon black (Denka Black Li-100, Denka Ltd.) (0.66 g) and dehydrated ethanol (2 g) were added and ball-milled at 1100 rpm for one hour. Then ethanol was evaporated, resulting in o-PbF_2@C. These processes were conducted in a dry chamber (Daikin Ltd., dew-point of -60 °C). Then o-PbF_2@C was heated in an Ar flow at 350 °C for 30 minutes to change the orthorhombic structure to a cubic structure, resulting in c-PbF_2@C. The low temperature of 350 °C was chosen to minimize agglomeration of particles.

Figures S23a, S23b and S23c show SEM images of o-PbF_2(BM), o-PbF_2@C and c-PbF_2@C, respectively. The sizes of particles in the three samples are similar. Figures S24a and S24b show XRD patterns of o-PbF_2@C and c-PbF_2@C (c). The patterns indicate that o-PbF_2@C and c-PbF_2@C have orthorhombic and cubic structures, respectively.

o-PbF_2@C (0.5 g) or c-PbF_2@C (0.5 g), PVDF (KF polymer L#1120, Kureha Ltd.) (0.09g) and an appropriate amount of *N*-methylpyrrolidone were mixed to make a slurry. An Al foil (thickness of 20 μm) was painted with the slurry and dried at 130 °C in vacuum, resulting in composite electrodes of o-PbF_2@C or c-PbF_2@C.

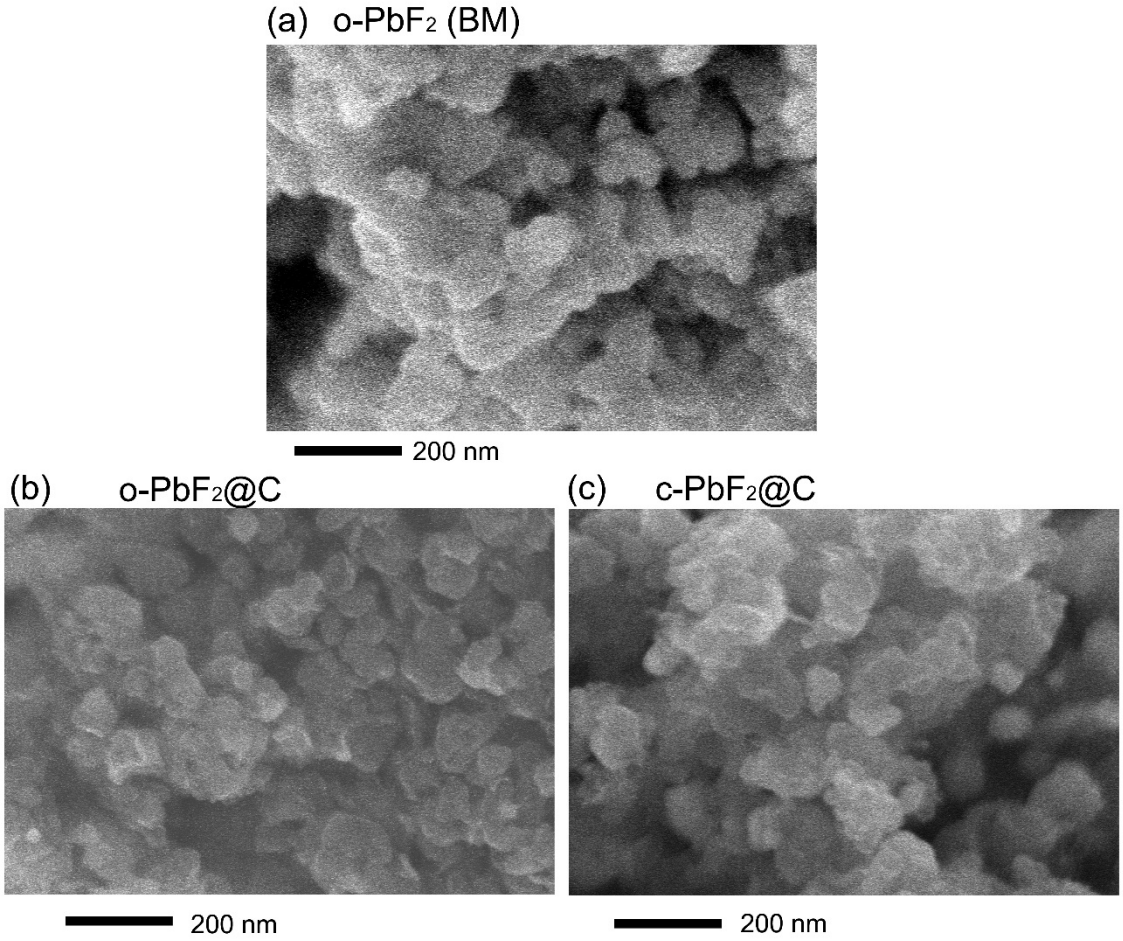

Fig. S23 SEM images of o-PbF_2(BM) (a), o-PbF_2@C (b) and o-PbF_2@C (c).

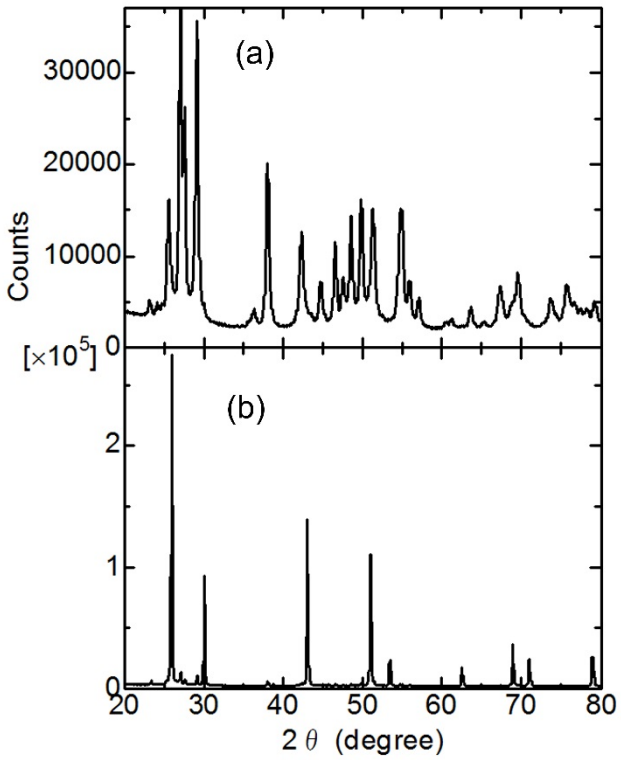

Fig. S24 XRD patterns of o-PbF_2@C (a) and c-PbF_2@C (b).

7-2 Constant current test

Changes in the potential of composite electrodes of o-PbF_2@C or c-PbF_2@C in the electrolyte were studied during application of a constant current at 1/40 C. A three-electrode electrochemical cell (EC Frontier Ltd.) was used with a platinum foil (a counter electrode) and a silver rod (a reference electrode). The silver rod was immersed in acetonitrile with 0.1 M silver nitrate and 0.1 M tetraethylammonium perchlorate (0.587 V vs. standard hydrogen electrode (SHE)).

Figure S25 shows results for o-PbF_2@C. Figure S25a shows a plot of the potential against capacity. During discharging (defluorination), the potential first decreased and then increased to make a plateau, as indicated by violet arrows. These features are probably due to desorption-induced dissolution of o-PbF_2 and subsequent deposition of Pb (Fig. 10c in the main text). Since deposition of Pb occurs at 0 V vs Pb (about -0.8 V in Fig. S25a), the potential increased to about -0.8 V as deposition of Pb proceeded. In addition, electrical contact between o-PbF_2 particles and a carbon conductive assistant became better with deposition of Pb, which reduced the overpotential. The capacity of discharging was almost the same as the theoretical value (219 mAh g^{-1}), but the capacity of charging was less than 80% of the theoretical value. The dip and plateau in Fig. S25a were not observed in the second and third cycles, and capacity faded quickly. Improvement of cycle performance of the electrode is a future subject.

Figures S25b, S25c and S25d show XRD patterns of the pristine electrode, the electrode after full discharging (defluorination) and the electrode after full charging, respectively. The results show that o-PbF_2 almost completely changed to Pb after full discharging. However, XRD peaks of o-PbF_2 or c-PbF_2 were not observed after full charging. This is consistent with the formation of an amorphous phase of PbF_2 and desorption of Pb during charging, as suggested by the results shown in Fig. 6d in the main text.

Figures S25e, S25f and S25g show XPS spectra of the pristine electrode, the electrode after full discharging and the electrode after full charging, respectively. Two peaks corresponding to Pb^{2+} (PbF_2) were seen around 139 and 144 eV in Fig. S25e. After full discharging, two peaks of metal Pb were observed around 136.6 and 141.5 eV, indicating defluorination. After charging, peaks corresponding to Pb^{2+} appeared again, suggesting oxidation reaction.

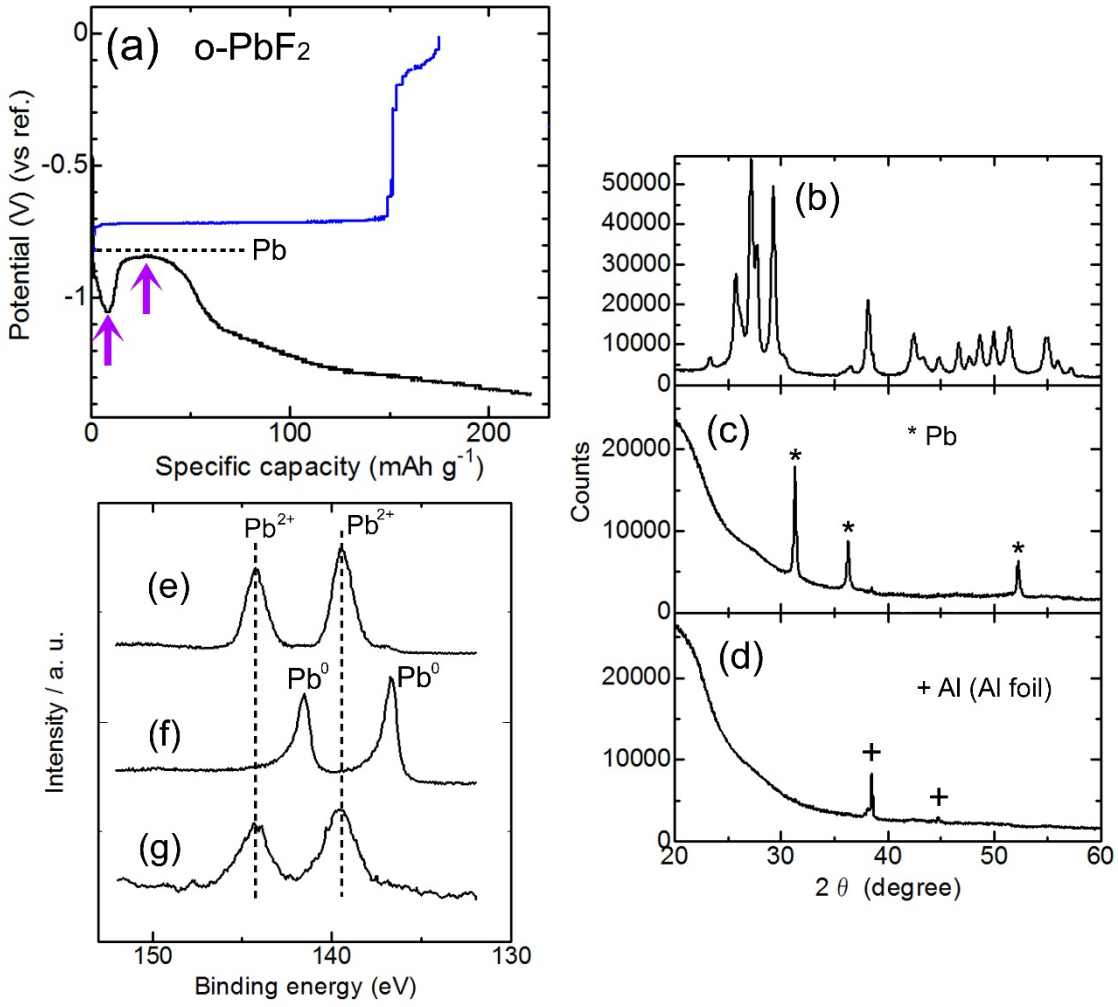

Fig. S25 Constant current test of an o-PbF_2@C composite electrode. (a) shows a plot of the potential of the electrode against capacity. (b), (c) and (d) show XRD patterns of the pristine electrode and the electrodes after full discharging (defluorination) and after full charging, respectively. (e), (f) and (g) show XPS spectra of the pristine electrode and the electrodes after full discharging (defluorination) and after full charging, respectively.

Figure S26 show results for c-PbF_2@C. Figure S26a shows a plot of the potential of the electrode against capacity. The potential decreased almost monotonously, being different from the results for o-PbF_2@C shown in Fig. S25a. This is because desorption-induced dissolution of c-PbF_2 and subsequent deposition of Pb (Fig. 10c in the main text) did not occur. The capacity of discharging was almost the same as the theoretical value (219 mAh g^{-1}). However, the capacity of charging was about 60% of the theoretical value and capacity faded quickly after the second cycle. Effects of defluorination mechanisms on electrochemical performance of composite electrodes were clearly observed as different features of potential plots between o-PbF_2@C (Fig. S25a) and c-PbF_2@C (Fig. S26a).

Figures S26b, S26c and S26d show XRD patterns of the pristine electrode and the electrodes after full discharging and after full charging, respectively. The results show that c-PbF_2 almost completely changed to Pb after full discharging. XRD peaks of o-PbF_2 or c-PbF_2 were not observed after charging. The results suggest the formation of an amorphous phase of PbF_2 and/or desorption of Pb during charging.

Figures S26e, S26f and S26g show XPS spectra of the pristine electrode and the electrodes after full discharging and after full charging, respectively. Two peaks corresponding to Pb^{2+} (PbF_2) are seen in Fig. S26e, and two peaks of metal Pb are seen after discharging in Fig. S26f. After charging, peaks corresponding to Pb^{2+} appeared again, suggesting oxidation reaction.

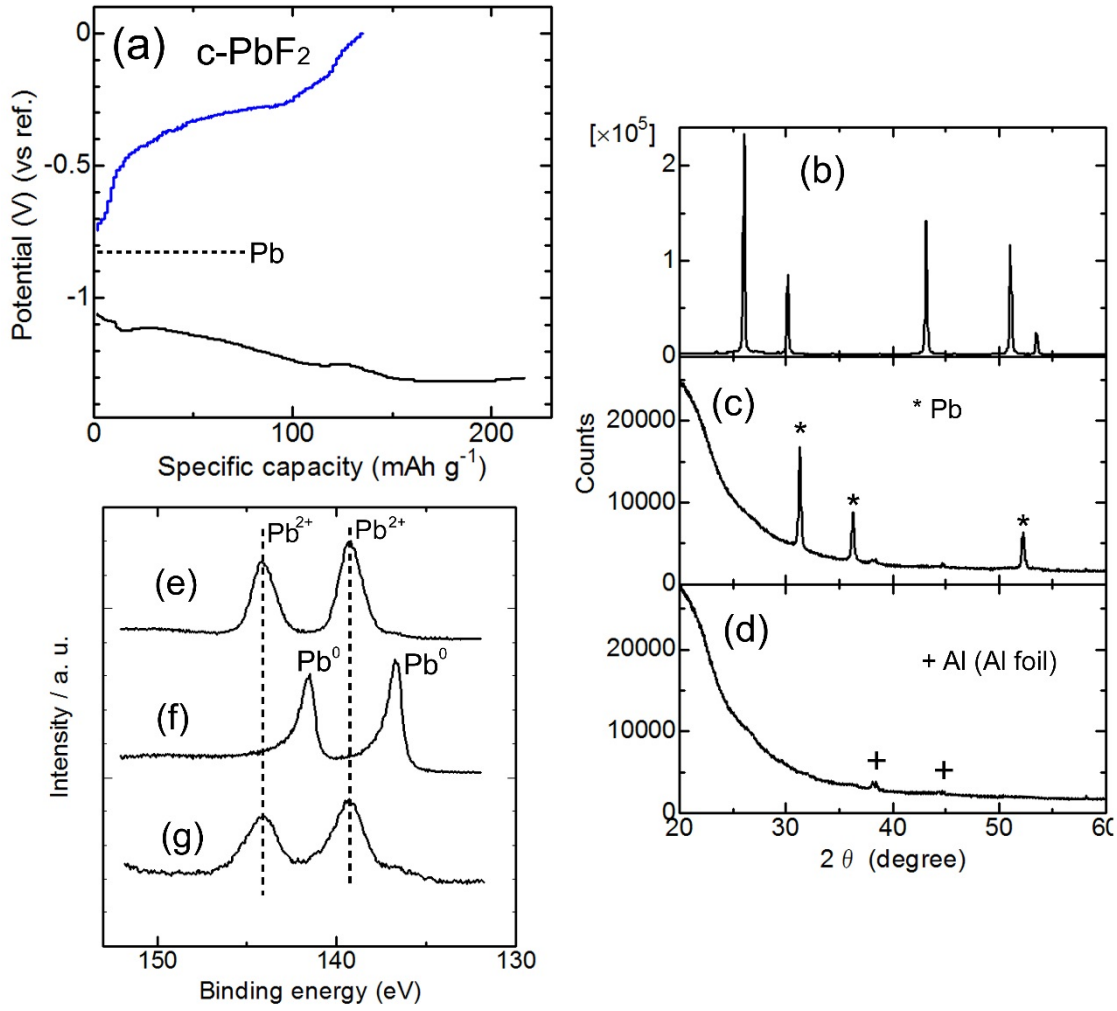

Fig. S26 Constant current test of a c-PbF_2@C composite electrode. (a) shows a plot of the potential of the electrode against capacity. (b), (c) and (d) show XRD patterns of the pristine electrode and the electrodes after full discharging and after full charging, respectively. (e), (f) and (g) show XPS spectra of the pristine electrode and the electrodes after full discharging and after full charging, respectively.

8. Structures of o-PbF_2, c-PbF_2 and Pb

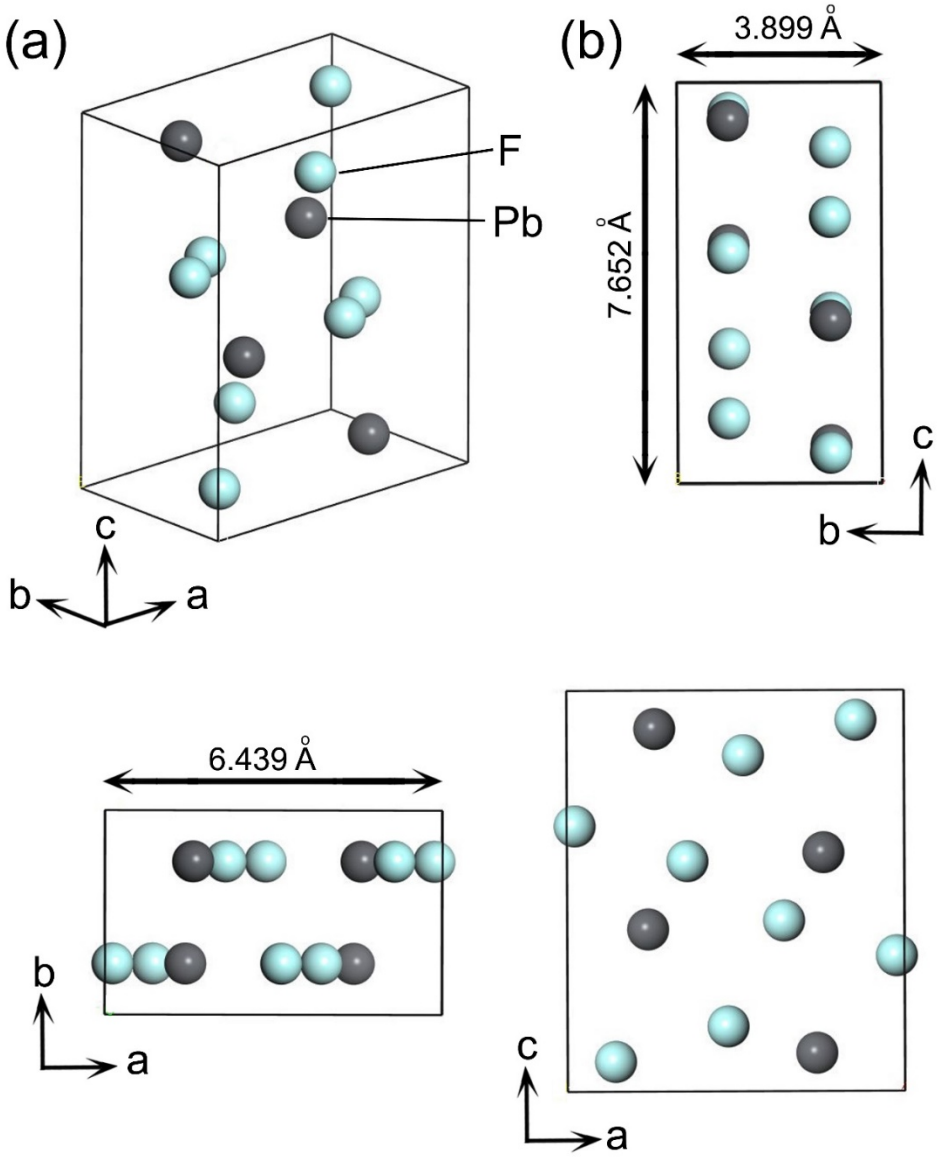

Fig. S27 Structure of o-PbF_2.

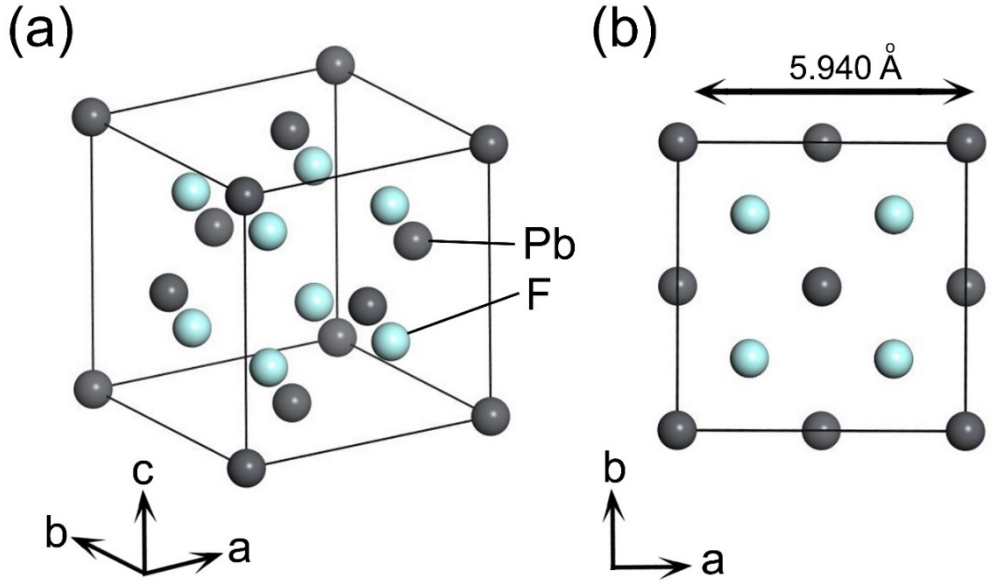

Fig. S28 Structure of c-PbF_2.

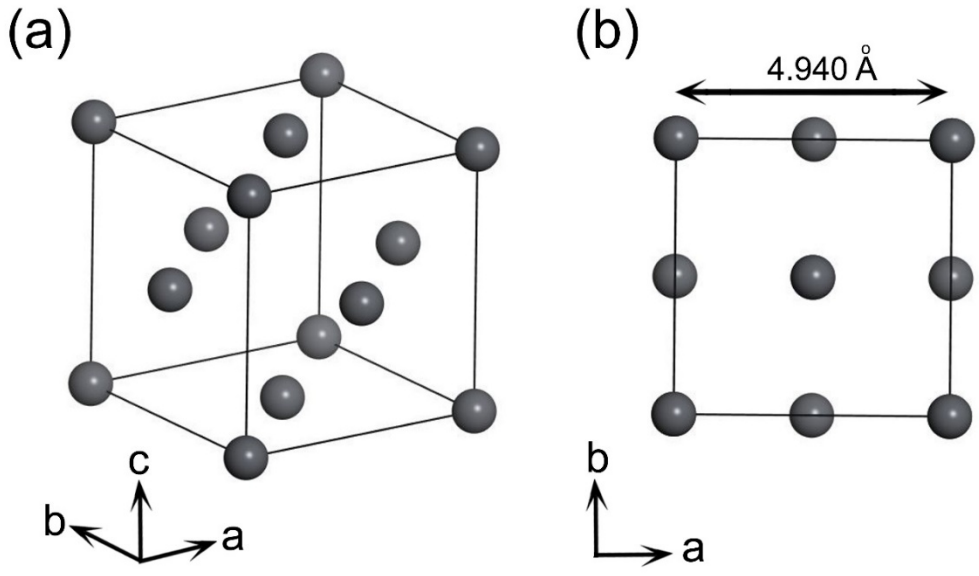

Fig. S29 Structure of Pb.

9. Increases in apparent volumes of c-PbF_2 particles during defluorination immediately after construction of a cell

As shown in Figs. 5, 6 and 9 in the main text, apparent volumes of o-PbF_2 and c-PbF_2 particles increased during desorption of F^- at -0.25 V. In these measurements, cell voltages (E_{WE}) were kept above -0.25 V for 120 hours for o-PbF_2/gold (Fig. 3a in the main text) and 41 hours for c-PbF_2/gold (Fig. 8a in the main text) before desorption of F^- started at -0.25 V, during which time dissolution of significant amounts of o-PbF_2 and c-PbF_2 should have occurred, resulting in Pb^{2+} ions in the solutions. At -0.25 V, the rate of deposition of Pb increased and it is thought that some Pb was deposited on partly defluorinated o-PbF_2 and c-PbF_2 particles, resulting in increases in apparent volumes of the particles. To study whether apparent volumes of particles increase or not without the effect of Pb deposition, changes in apparent volumes of c-PbF_2 particles were measured within three hours from construction of a cell in order to minimize dissolution of c-PbF_2 and deposition of Pb. o-PbF_2 was not used because desorption-induced dissolution and subsequent deposition of Pb occur at -0.25 V if o-PbF_2 is used.

Figures S30a and S30b show confocal CCD images of c-PbF_2/gold just after the cell was assembled and after it was kept at -0.25 V for one hour to induce desorption of F^- from c-PbF_2 particles, respectively. The image in Fig. S30a is the same as that in Fig. S19a, but the image in Fig. S30b (-0.25 V, 1 hour) is not the same image as that in Fig. S 19b (-0.25 V, 4 hours). Zoomed images of areas indicated by rectangles in Figs. S30a and 30b are shown in Figs. S31a and S31b, respectively. In Fig. S30b, small particles and small structures indicated by numbers became dark, indicating that defluorination occurred. Since these measurements were conducted within three hours from construction of the cell, deposition of Pb on the gold substrate was not observed by color change (see Fig. S31). Figures S30c and S30d show 3D images corresponding to Figs. S30a and S30b, respectively. The apparent volumes of the particles are summarized in Table SI. It is difficult to measure volumes of dark structures 2 and 4 in Fig. S30b because these are parts of large particles, and these parts are excluded in Table SI. It is shown that volumes of all particles increased after keeping the sample at 0.25 V for one hour. Particle 7 shows a large volume change of 23.3 μm^3, which is not likely to be due to deposition of Pb considering the short time taken for the present experiments. Thus, we think that apparent volumes of c-PbF_2 particles increase during desorption of F^- even if deposition of Pb does not occur.

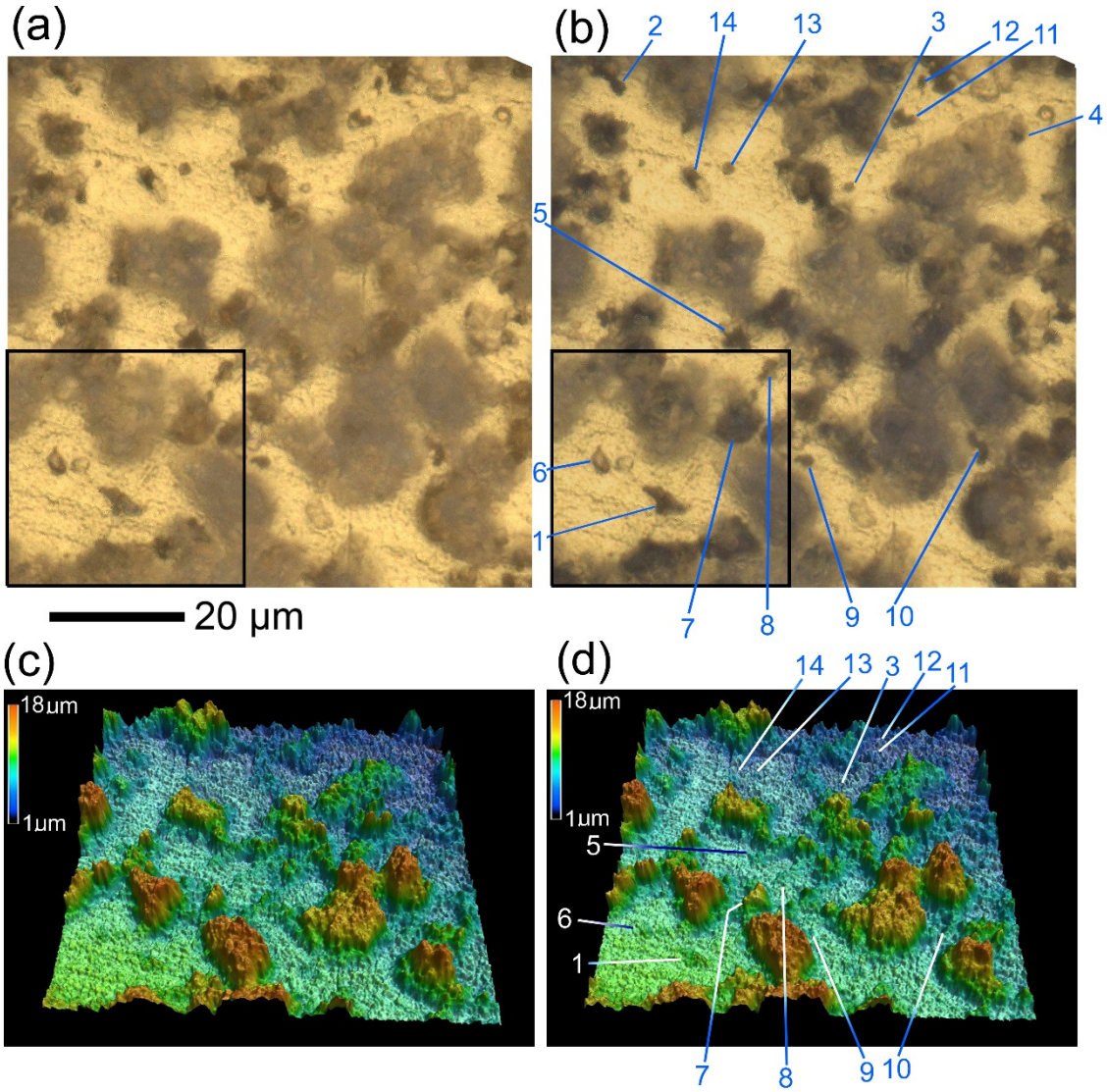

Fig. S30 Changes in apparent volumes of c-PbF_2 particles at -0.25 V within three hours from construction of the cell. Confocal CCD images of c-PbF_2/gold at (a) OCV and (b) after the sample was kept at -0.25 V for one hour. 3D images of c-PbF_2/gold at (c) OCV and (d) after the sample was kept at -0.25 V for one hour.

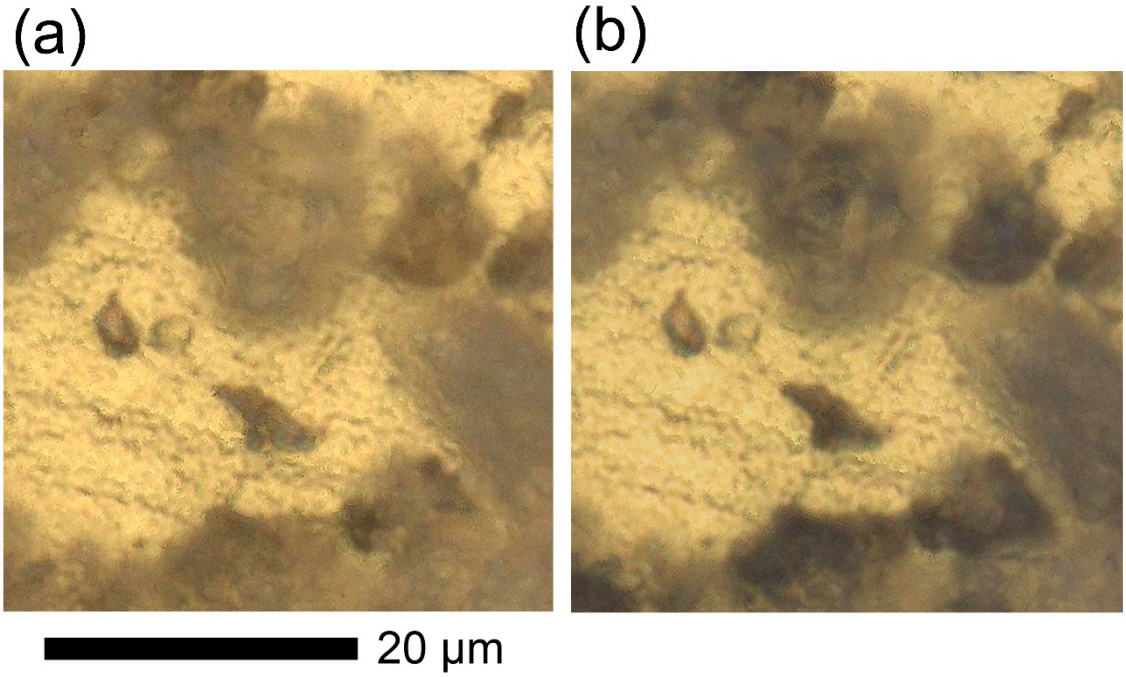

Fig. S31 Zoomed confocal CCD images of c-PbF_2/gold at (a) OCV and (b) after the sample was kept at -0.25 V for one hour. (a) and (b) correspond to areas shown by rectangles in Figs. S30a and S30b, respectively.

Table SI Changes in apparent volumes of c-PbF_2 particles above gold after being kept at -0.25 V for one hour. Particle numbers correspond to those in Fig. 30.

particle nuumber	1	3	5	6	7	8	9	10	11	12	13	14
apparent volume above gold at OCV (um^3)	9.1	0.6	3.1	1.65	62.3	1.9	0.7	5	0.2	0.2	0.4	7.2
apparent volume above gold at -0.25 V (1 h.) (um^3)	12.1	2.3	6.1	3.1	85.6	5.2	1.1	9.1	1.4	2.5	0.9	8.6

To further confirm the observed volumetric changes of c-PbF_2 particles without deposition of Pb, a new cell was constructed using a new c-PbF_2/gold sample and similar measurements were conducted again. Figures S32a and S32b show confocal CCD images of c-PbF_2/gold at OCV and after being kept at -0.25 V for one hour, respectively. Zoomed images of areas indicated by rectangles in Figs. S32a and 32b are shown in Figs. S33a and 33b, respectively. Small c-PbF_2 particles indicated by numbers became dark after the sample was kept at -0.25 V (Fig. S32b), indicating defluorination. Apparent volumes of the particles were measured at OCV (Figs. S32a and S32c) and after the sample was kept

at -0.25 V (Figs. S32b and S32d). Measurements were conducted within three hours from construction of the cell. Apparent volumes increased again after keeping the sample at -0.25 V, while deposition of Pb on the gold substrate was not observed (see Fig. S33). The results are summarized in table SII.

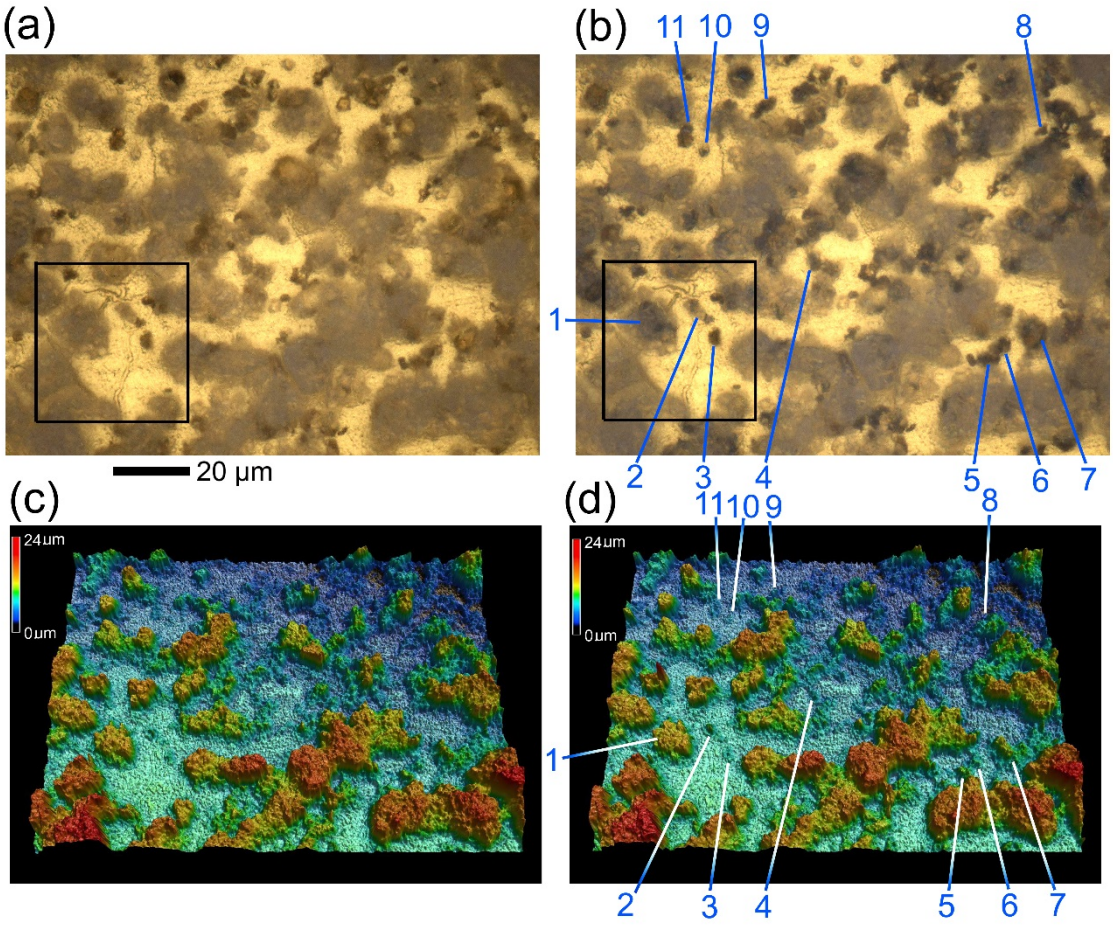

Fig. S32 Changes in apparent volumes of c-PbF_2 particles at -0.25 V within three hours from construction of the cell. Confocal CCD images of c-PbF_2/gold at (a) OCV and (b) after the sample was kept at -0.25 V for one hour. 3D images of c-PbF_2/gold at (c) OCV and (d) after the sample was kept at -0.25 V for one hour.

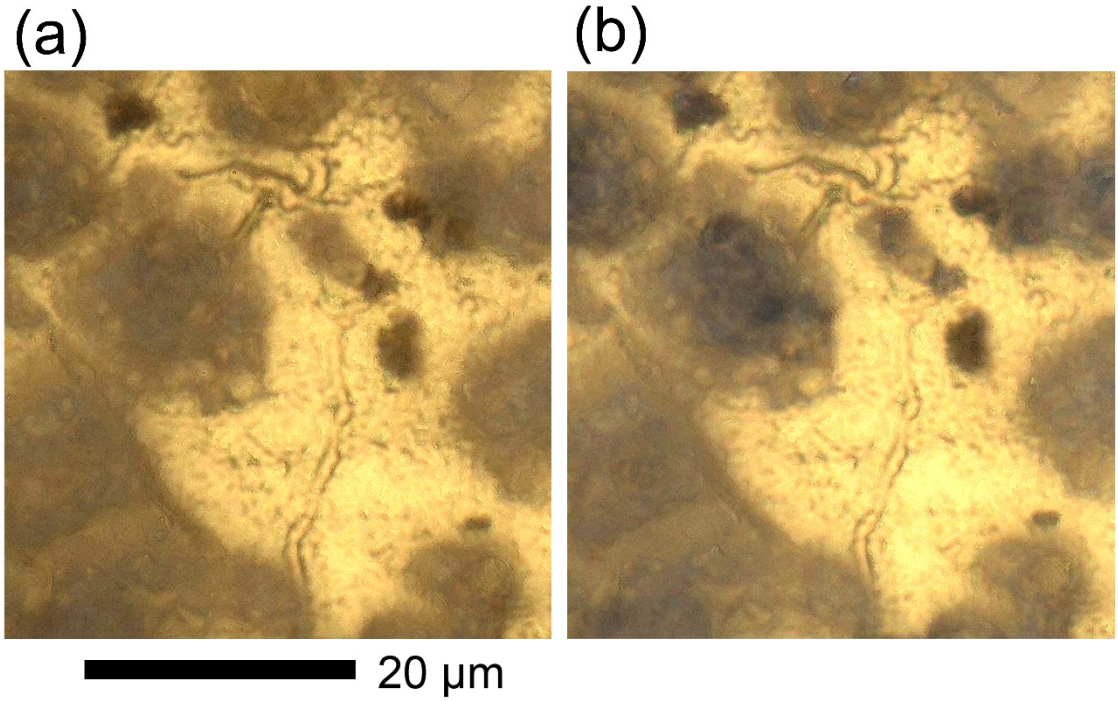

Fig. S33 Zoomed confocal CCD images of c-PbF_2/gold at (a) OCV and (b) after the sample was kept at -0.25 V for one hour. (a) and (b) correspond to areas shown by rectangles in Figs. S32a and S32b, respectively.

Table SII Changes in apparent volumes of c-PbF_2 particles above gold after being kept at -0.25 V for one hour. Particle numbers correspond to those in Fig. 32.

particle nuumber	1	2	3	4	5	6	7	8	9	10	11
apparent volume above gold at OCV (μm^3)	494	11.4	9.2	10.2	30.9	9.7	12.6	7.0	13.5	1.3	10.1
apparent volume above gold at -0.25 V (1 h.) (μm^3)	522	21.2	10.7	11.2	37	18.3	18.1	9.3	15.7	7.2	12.1

10. Comparison of o-PbF_2/gold (-0.25 V, 54 hours), o-PbF_2/gold (-0.25 V, 74 hours) and c-PbF_2/gold (-0.25 V, 70 hours).

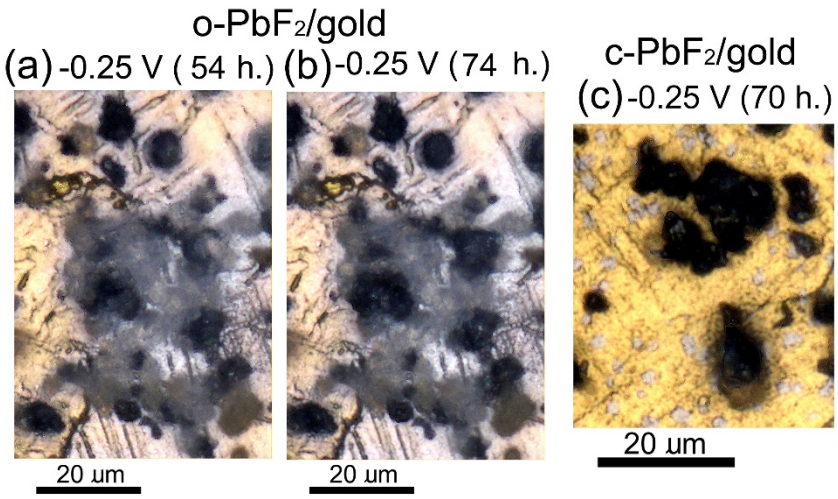

Fig. S34 Comparison of o-PbF_2/gold and c-PbF_2/gold, which were kept at -0.25 V for similar durations. (a) and (b) show confocal CCD images of o-PbF_2/gold after being kept at -0.25 V for 54 hours and 74 hours, respectively. (c) shows a confocal CCD image of c-PbF_2/gold after being kept at -0.25 V for 70 hours (the same as Fig. 9c in the main text). It is seen that deposition of Pb on the gold substrate is more significant for o-PbF_2/gold than for c-PbF_2/gold.